



This is a repository copy of *A novel reformulation of the Theory of Critical Distances to design notched metals against dynamic loading*.

White Rose Research Online URL for this paper:
<http://eprints.whiterose.ac.uk/90841/>

Version: Accepted Version

Article:

Yin, T., Tyas, A., Plekhov, O. et al. (2 more authors) (2015) A novel reformulation of the Theory of Critical Distances to design notched metals against dynamic loading. *Materials & Design*, 69. 197 - 212. ISSN 0261-3069

<https://doi.org/10.1016/j.matdes.2014.12.026>

Reuse

Unless indicated otherwise, fulltext items are protected by copyright with all rights reserved. The copyright exception in section 29 of the Copyright, Designs and Patents Act 1988 allows the making of a single copy solely for the purpose of non-commercial research or private study within the limits of fair dealing. The publisher or other rights-holder may allow further reproduction and re-use of this version - refer to the White Rose Research Online record for this item. Where records identify the publisher as the copyright holder, users can verify any specific terms of use on the publisher's website.

Takedown

If you consider content in White Rose Research Online to be in breach of UK law, please notify us by emailing eprints@whiterose.ac.uk including the URL of the record and the reason for the withdrawal request.



eprints@whiterose.ac.uk
<https://eprints.whiterose.ac.uk/>

Please, cite this paper as: Yin, T., Tyas, A., Plekhov, O., Terekhina, A., Susmel, L. A novel reformulation of the Theory of Critical Distances to design notched metals against dynamic loading. *Materials and Design*, 69, pp. 197–212, 2015.

A novel reformulation of the Theory of Critical Distances to design notched metals against dynamic loading

T. Yin¹, A. Tyas¹, O. Plekhov², A. Terekhina² and L. Susmel¹

¹Department of Civil and Structural Engineering, The University of Sheffield, Sheffield S1 3JD, United Kingdom

²Institute of Continuous Media Mechanics UB RAS - 1, Ak. Koroleva str., 614013 Perm, Russia

Corresponding Author: Prof. Luca Susmel
Department of Civil and Structural Engineering
The University of Sheffield, Mappin Street, Sheffield, S1 3JD, UK
Telephone: +44 (0) 114 222 5073
Fax: +44 (0) 114 222 5700
e-mail: l.susmel@sheffield.ac.uk

Abstract

The most remarkable peculiarity of the so-called Theory of Critical Distances (TCD) is that, independently from the level of ductility characterising the considered material, this method allows the strength of notched/cracked components to be estimated accurately by simply post-processing the entire linear-elastic stress fields acting on the material in the vicinity of the stress concentrator being designed. By taking as a starting point the above idea, in the present study the TCD was reformulated to make it suitable for predicting the strength of notched metallic materials subjected to dynamic loading. The accuracy and reliability of the proposed reformulation of the TCD was checked against a number of experimental results generated by testing, under different loading/strain rates, notched cylindrical samples of aluminium alloy 6063-T5, titanium alloy Ti-6Al-4V, aluminium alloy AlMg6, and an AlMn alloy. To further validate the proposed design method also different data sets taken from the literature were considered. Such an extensive validation exercise allowed us to prove that the proposed reformulation of the TCD is successful in predicting the dynamic strength of notched metallic materials, this approach proving to be capable of estimates falling within an error interval of $\pm 20\%$. Such a high level of accuracy is certainly remarkable, especially in light of the fact that it was reached without the need for explicitly modelling the stress vs. strain dynamic behaviour of the investigated ductile metals. This suggests that the proposed design methodology has the potential of changing the way notched metallic components are designed against dynamic loading in situations of practical interest.

Keywords: Theory of Critical Distances, notches, dynamic fracture, metallic materials.

1. Introduction

In situations of practical interest (such as car crash, forging & rolling, sudden impacts, etc.), engineering components and structures have to be designed to withstand high rate of loading. In this context, examination of the state of the art suggests that, since about the beginning of the last century, the international scientific community has made a tremendous effort to understand and model the mechanical/cracking behaviour of engineering materials subjected to high rate of loading. This large body of work shows that this problem has been extensively addressed by tackling it both from an experimental and a theoretical angle. Back in 1914, Hopkinson [1] developed the device which became known as Hopkinson Pressure Bar, suitable for measuring the impulse and pressure generated by the impact of bullets or the detonation of explosives. Thirty years later, Davies [2] revisited Hopkinson's pressure bar developing the theoretical basis of the wave propagation analysis required to understand the results, and introducing electronic measurement of the stress waves in the bar. In 1949, Kolsky [3] developed what has become known as the Split-Hopkinson Pressure Bar or Kolsky bar test, in which a small sample of material is sandwiched between the ends of two long cylindrical bars. When an axial dynamic load is induced in one bar, this partially reflects and partially transmits through the sample. By analysing the incident, reflected and transmitted waves, Kolsky showed that it was possible to determine the dynamic stress, strain and strain rate which the specimen experienced during the loading. This pioneering work has been followed by a multitude of subsequent investigations further confirming the validity of Kolsky's findings, that, generally, the mechanical behaviour of materials is strain rate dependent. In this context, a number of experimental studies [4-10] have proven that, at room temperature, the failure stress tends to increase with the increase of the loading/strain rate, this holding true both for aluminium alloys and steels.

After the advent of Linear Elastic Fracture Mechanics (LEFM), accurate investigations were carried out also to study the existing relationship between material fracture toughness and rate of the applied loading. As to this aspect, examination of the state of the art [10-12]

Please, cite this paper as: Yin, T., Tyas, A., Plekhov, O., Terekhina, A., Susmel, L. A novel reformulation of the Theory of Critical Distances to design notched metals against dynamic loading. *Materials and Design*, 69, pp. 197–212, 2015.

suggests that, at room temperature, the fracture toughness can either decrease, increase, or remain constant as the Stress Intensity Factor (SIF) rate increases, this mainly depending on the microstructural features of the metallic material being investigated.

It is well known that under quasi-static loading, notches have a detrimental effect on the overall static strength of engineering materials. Accordingly, appropriate design methods have to be used to accurately design components experiencing stress concentration phenomena. In this context, it is recognised that the so-called Theory of Critical Distances (TCD) is the most effective tools which can be used by structural engineers to take into account the weakening effect of notches of all kinds. The fundamental idea on which the TCD is based was first proposed in about the middle of the last century to specifically estimate the high-cycle fatigue strength of notched components. In more detail, Neuber [13] suggested performing the high-cycle fatigue assessment of metals containing notches through an effective stress calculated by averaging the linear-elastic stress over a straight line emanating from the notch tip. A few years later, Peterson [14] observed that the problem could greatly be simplified by directly using, as effective stress, the linear-elastic stress evaluated at a given distance from the notch apex. In both Neuber's and Peterson's approach, this length scale parameter was treated as a material property. Late in the 1960s, Novozhilov [15, 16] has proven that Neuber's method could also be derived by using an elegant energy argument. In 1974, Whitney and Nuismer [17] showed that the TCD could be used to estimate the static strength of notched composite, the material critical length being directly determined through the LEFM fracture toughness and the ultimate tensile strength. Toward the end of the last century, Tanaka [18] and Taylor [19] have proven that the TCD could successfully be employed to estimate notch fatigue limits also by calculating the necessary critical distance via the threshold value of the stress intensity factor and the plain fatigue limit. Owing to its accuracy in assessing the detrimental effect of notches, in recent years, the TCD has gained new popularity being used to address a variety of structural integrity problems [20]. For instance, the TCD applied along with the so-called Modified Wöhler Curve Method was seen

Please, cite this paper as: Yin, T., Tyas, A., Plekhov, O., Terekhina, A., Susmel, L. A novel reformulation of the Theory of Critical Distances to design notched metals against dynamic loading. *Materials and Design*, 69, pp. 197–212, 2015.

to be capable of accurately designing notched components against multiaxial fatigue [21-23]. Recently, it was also proven that the TCD is successful in estimating the static strength of both ductile and brittle notched materials subjected to uniaxial as well as to multiaxial static loading [24-25]. Finally, Cicero et al. [26-28] have successfully used the TCD to model the effect of the notch sharpness on the apparent fracture toughness.

Independently from the structural integrity ambit in which it is used, the most important feature of the TCD is that this theory is seen to be capable of accommodating any kind of material non-linearities into a linear-elastic framework, this allowing the time and costs associated with the design process to be reduced remarkably [29]. Another important aspect which is worth being mentioned is that, by nature, the TCD can be calibrated by using pieces of experimental information generated via conventional testing equipment.

Owing to its unique features, the challenging aim of this paper is to reformulate the linear-elastic TCD to make it suitable for designing notched metallic components against dynamic loading, the material behaviour being, by nature, highly non-linear.

2. TCD and static assessment of notched components

As far as notched engineering materials subjected to quasi-static loading are concerned, the TCD postulates that the static strength of notched components can be estimated by directly post-processing the entire linear-elastic stress field acting on the material in the vicinity of the stress raiser being assessed. Examination of the state of the art suggests that, since about the middle of the last century, the above idea has been formalised (and validated through appropriate experimental investigations) in different ways which include the Point, the Line, the Area, and the Volume Method [20].

If attention is focussed on notches subjected to Mode I quasi-static loading, according to the TCD, breakage takes place as soon as a critical distance depending effective stress, σ_{eff} , becomes larger than the material inherent strength, σ_0 [24]. Therefore, the notched

Please, cite this paper as: Yin, T., Tyas, A., Plekhov, O., Terekhina, A., Susmel, L. A novel reformulation of the Theory of Critical Distances to design notched metals against dynamic loading. *Materials and Design*, 69, pp. 197–212, 2015.

component being designed is supposed to be capable of withstanding the applied loading as long as the following condition is assured:

$$\sigma_{\text{eff}} \leq \sigma_0 \quad (1)$$

One of the most interesting features of the TCD is that effective stress σ_{eff} can be estimated by adopting a simple linear-elastic constitutive law [19, 20], this holding true independently from the level of ductility characterising the material under investigation [24, 25]. This results in a great simplification of the design problem, allowing structural engineers to perform the required stress analysis via simple linear-elastic models done using commercial Finite Element (FE) software packages.

According to condition (1), to properly use the TCD in situations of practical interest, the second important information which is needed is the material inherent strength, σ_0 . As to the expected values for σ_0 , it is worth recalling here that the inherent strength equals the conventional ultimate tensile strength, σ_{UTS} , solely under particular circumstances, this mainly depending on the mechanical behaviour as well as on the microstructural features of the material being designed. In particular, when breakage is preceded by a certain amount of plastic deformation, σ_0 takes on a value which is larger than the ultimate tensile strength [20]. This obviously applies also to metallic materials [29], even if, for certain metals, σ_0 is seen to be so close to σ_{UTS} [24] that the TCD can successfully be used by simply taking $\sigma_0 = \sigma_{\text{UTS}}$. On the contrary, as far as brittle materials (such as ceramics [30]) or quasi-brittle materials (such as fibre composites [17]) are concerned, σ_0 is seen to be invariably equal to σ_{UTS} . Lastly, it should be noted that σ_0 is seen to be different from σ_{UTS} also in those situations where the presence of stress raisers leads to different failure mechanisms to those resulting in the breakage of the un-notched material [31]. These considerations clearly suggest that the most accurate way to estimate material inherent strength σ_0 is by running

Please, cite this paper as: Yin, T., Tyas, A., Plekhov, O., Terekhina, A., Susmel, L. A novel reformulation of the Theory of Critical Distances to design notched metals against dynamic loading. *Materials and Design*, 69, pp. 197–212, 2015.

appropriate experiments, the recommended experimental procedure for the determination of σ_o being explained below.

Turning back to the different formalisations of the TCD, effective stress σ_{eff} can be calculated according to either the Point Method (PM), the Line Method (LM), or the Area Method (AM) as follows [19]:

$$\sigma_{\text{eff}} = \sigma_y \left(\theta = 0, r = \frac{L}{2} \right) \quad (\text{PM}) \quad (2)$$

$$\sigma_{\text{eff}} = \frac{1}{2L} \int_0^{2L} \sigma_y(\theta = 0, r) \, dr \quad (\text{LM}) \quad (3)$$

$$\sigma_{\text{eff}} = \frac{2}{\pi L^2} \int_{-\pi/2}^{\pi/2} \int_0^L \sigma_1(\theta, r) \, r \, dr d\theta \quad (\text{AM}) \quad (4)$$

The meaning of the adopted symbols as well as of the effective stress calculated according to definitions (2), (3), and (4) is explained in Figures 1a to 1d.

Equations (2) to (4) show that, independently from the strategy adopted to determine σ_{eff} , the TCD makes use of a length scale parameter which can be estimated via the LEFM plane strain fracture toughness, K_{Ic} , and the material inherent strength, σ_o , as follows [20]:

$$L = \frac{1}{\pi} \left(\frac{K_{Ic}}{\sigma_o} \right)^2 \quad (5)$$

According to definition (5), as soon as K_{Ic} is known from the experiments, the determination of critical distance L is straightforward solely for those materials for which inherent material strength σ_o is invariably equal to the ultimate tensile strength, σ_{UTS} . On the contrary, when $\sigma_o \neq \sigma_{UTS}$, the only way to determine L is by testing samples containing notches of different sharpness [24, 25]. This procedure is summarised in Figure 1e: as postulated by the PM, the

Please, cite this paper as: Yin, T., Tyas, A., Plekhov, O., Terekhina, A., Susmel, L. A novel reformulation of the Theory of Critical Distances to design notched metals against dynamic loading. *Materials and Design*, 69, pp. 197–212, 2015.

coordinates of the point at which the two linear-elastic stress-distance curves, plotted in the incipient failure condition, intersect each other allow length scale parameter L and inherent strength σ_0 to be estimated directly. To conclude, it is worth observing that such an experimental procedure based on notches of different sharpness was seen to be very accurate also to estimate the LEFM plane strain fracture toughness [32]. In fact, after determining both L and σ_0 according to the procedure schematically depicted in Figure 1e, K_{Ic} can directly be estimated via Eq. (5), the LEFM plane strain fracture toughness obviously becoming the unknown variable in the problem.

3. Reformulating the TCD to design notched materials against dynamic loading

As briefly mentioned in the previous section, the TCD postulates that the static assessment has to be performed by post-processing the entire stress field damaging the so-called process zone (i.e., that material portion controlling the overall strength of the component being assessed) [20]. Through length scale parameter L , the size of the process zone depends mainly on: (i) material microstructural features, (ii) local micro-mechanical properties, and (iii) characteristics of the processes resulting in the final breakage [20]. Examination of the state of the art [3-11] suggests that, in general, the mechanical response, mechanical properties and cracking behaviour of metallic materials subjected to dynamic loading are different from the ones observed under quasi-static loading. If these universally accepted concepts are reinterpreted according to the TCD's philosophy, one may argue that, since both the dynamic failure stress, σ_f , and the dynamic fracture toughness, K_{Id} , vary as the applied load/strain/displacement rate increases, in the same way also the inherent strength, σ_0 , and the length scale parameter, L , have to vary. In particular, if \dot{Z} is used to denote either the loading rate, \dot{F} , the strain rate, $\dot{\epsilon}$, the displacement rate, $\dot{\Delta}$, or the Stress Intensity Factor (SIF) rate, \dot{K}_I , the effect of the dynamic loading on both the failure stress, σ_f , and the fracture toughness, K_{Id} , can be expressed as follows:

Please, cite this paper as: Yin, T., Tyas, A., Plekhov, O., Terekhina, A., Susmel, L. A novel reformulation of the Theory of Critical Distances to design notched metals against dynamic loading. *Materials and Design*, 69, pp. 197–212, 2015.

$$\sigma_f(\dot{Z}) = f_{\sigma_f}(\dot{Z}) \quad (6)$$

$$K_{ld}(\dot{Z}) = f_{K_{ld}}(\dot{Z}) \quad (7)$$

where $f_{\sigma_f}(\dot{Z})$ and $f_{K_{ld}}(\dot{Z})$ are functions which can be either estimated experimentally or derived theoretically. The strategy we propose to define such functions will be discussed in the next section in great detail.

Since, under static loading, σ_o is seen to be proportional to σ_{UTS} [20], the hypothesis can be formed that, similar to the dynamic failure stress, Eq. (6), also the inherent material strength varies with \dot{Z} , i.e.:

$$\sigma_o(\dot{Z}) = f_{\sigma_o}(\dot{Z}), \quad (8)$$

where, again, function $f_{\sigma_o}(\dot{Z})$ can be either estimated experimentally or derived theoretically. If this assumption is correct, then, in the most general case, also the length scale parameter has to change with \dot{Z} . Therefore, by rewriting definition (5) for the dynamic case, L can directly be expressed as:

$$L(\dot{Z}) = \frac{1}{\pi} \left[\frac{K_{ld}(\dot{Z})}{\sigma_o(\dot{Z})} \right]^2 = f_L(\dot{Z}) \quad (9)$$

To design notched materials against dynamic loading, according to definitions (2), (3), and (4), effective stress σ_{eff} can now be rearranged as follows:

Please, cite this paper as: Yin, T., Tyas, A., Plekhov, O., Terekhina, A., Susmel, L. A novel reformulation of the Theory of Critical Distances to design notched metals against dynamic loading. *Materials and Design*, 69, pp. 197–212, 2015.

$$\sigma_{\text{eff}}(\dot{Z}) = \sigma_y \left(\theta = 0, r = \frac{L(\dot{Z})}{2} \right) \quad (\text{PM}) \quad (10)$$

$$\sigma_{\text{eff}}(\dot{Z}) = \frac{1}{2L(\dot{Z})} \int_0^{2L(\dot{Z})} \sigma_y(\theta = 0, r) \, dr \quad (\text{LM}) \quad (11)$$

$$\sigma_{\text{eff}}(\dot{Z}) = \frac{2}{\pi L(\dot{Z})^2} \int_{-\pi/2}^{\pi/2} \int_0^{L(\dot{Z})} \sigma_1(\theta, r) \, r \, dr d\theta \quad (\text{AM}) \quad (12)$$

where, as postulated by the TCD [20], the stress analysis is still done by using a simple linear-elastic constitutive law. In other words, the hypothesis is formed that the behaviour of notched metallic materials subjected to dynamic loading can directly be modelled via $\sigma_0(\dot{Z})$ and $L(\dot{Z})$ without taking into account the actual dynamic stress vs. strain response of the material being assessed.

Turning back to the design issue, according to the assumptions made above, notched components undergoing in-service dynamic loading are then supposed not to fail as long as the following conditions is assured:

$$\sigma_{\text{eff}}(\dot{Z}) \leq \sigma_0(\dot{Z}), \quad (13)$$

the dynamic safety factor, v_D , taking on the following value:

$$v_D = \frac{\sigma_0(\dot{Z})}{\sigma_{\text{eff}}(\dot{Z})} \geq 1 \quad (14)$$

Having reformulated the TCD to make it suitable for designing notched metals against dynamic loading, it is useful to recall here that, back in the 90s, Morozov and Petrov have proposed to estimate the dynamic strength of cracked brittle materials according to the so-

Please, cite this paper as: Yin, T., Tyas, A., Plekhov, O., Terekhina, A., Susmel, L. A novel reformulation of the Theory of Critical Distances to design notched metals against dynamic loading. *Materials and Design*, 69, pp. 197–212, 2015.

called Structural-Time Criterion [33, 34]. If critical distance L is calculated via definition (5) independently from the rate of the applied loading, this failure criterion can be rewritten (according to the symbols adopted in the present paper) as follows:

$$\frac{1}{\tau} \int_{T_f - \tau}^{T_f} \frac{1}{2L} \int_0^{2L} \sigma_y(\theta = 0, r, t) \, dr \, dt \leq \sigma_{UTS} \quad (15)$$

where t is time, T_f is the time to failure, and τ is the so-called incubation time (which is treated as a material property [33, 34]). By comparing criterion (15) to the effective stress determined in terms of the LM, Eq. (3), the existing similarities between Morozov and Petrov's approach and the TCD become evident. In particular, the Structural-Time Criterion postulates that the strength of a cracked material subjected to dynamic loading can be brought back to the static case by simply averaging over time the LM's effective stress, the temporal integration domain being defined via time-related material constant τ . In other words, in Morozov and Petrov's criterion, the required critical distance is kept constant and equal to its value determined under quasi-static loading, the effect of the dynamic loading being assessed via the incubation time, τ . The reformulation of the TCD proposed in the present paper assumes instead that both the reference material strength, Eq. (8), and the size of the process zone, Eq. (9), vary as the rate of the applied loading increases. This assumption can be justified by observing that, in metallic materials, the micro-mechanisms resulting in the formation of the fracture surface are seen to change as the rate of the applied loading increases, this resulting in a variation of the morphology of the fracture surface itself [37-40]. As recalled above, according to the TCD's *modus operandi*, the size of the process zone depends mainly on the characteristics of those processes resulting in the final fracture [20]. Therefore, since the microstructural mechanisms leading to dynamic breakage vary as the loading rate increases, the size of the process zone is expected to change accordingly. This phenomenon is modelled in the proposed reformulation of the TCD by forming the

Please, cite this paper as: Yin, T., Tyas, A., Plekhov, O., Terekhina, A., Susmel, L. A novel reformulation of the Theory of Critical Distances to design notched metals against dynamic loading. *Materials and Design*, 69, pp. 197–212, 2015.

hypothesis that critical distance has to vary as the loading/strain/displacement rate increases, Eq. (9).

As far as critical length based approaches are concerned, it is worth recalling here also that the closed form approach to describe the “inertia” of fracture and introduce the characteristic length and time into the fracture mechanics problem was also proposed by Naimark and Plekhov [39, 40]. In this approach, the characteristic length and characteristic time of fracture were introduced based on the analysis of self-similar solutions of constitutive equations describing the defect evolution. It was shown that the processes resulting in the final breakage are accompanied by the collective modes of defect ensemble, which develop as instabilities with the blow-up kinetics localised on the spectrum of spatial scales. The Naimark and Plekhov’s description includes the discrete spectrum of critical distances considered as characteristics of both material structure and loading conditions. Each critical distance has own critical (incubation) time and can be realised under corresponding loading conditions [40].

Turning back to the new reformulation of the TCD proposed in the present paper, it is possible to conclude by observing that, owing to the complexity of the reasoning on which the devised design method is based, a set of appropriate experimental results is obviously required to check the validity of the formed hypotheses. However, before performing such a validation exercise, the next step in the development of the theory is rewriting functions $f_{\sigma_f}(\dot{Z})$, $f_{\sigma_o}(\dot{Z})$, $f_{K_{Id}}(\dot{Z})$, and $f_L(\dot{Z})$ in explicit form. This will be done in the next section.

4. Defining the governing equations

In order to find appropriate mathematical laws suitable for expressing functions $f_{\sigma_f}(\dot{Z})$, $f_{\sigma_o}(\dot{Z})$, $f_{K_{Id}}(\dot{Z})$, and $f_L(\dot{Z})$ in explicit form, a number of experimental data were selected from the technical literature. The log-log diagrams reported in Figure 2 show the way both engineering failure strength σ_f and dynamic fracture toughness K_{Id} vary as \dot{Z} increases. The

Please, cite this paper as: Yin, T., Tyas, A., Plekhov, O., Terekhina, A., Susmel, L. A novel reformulation of the Theory of Critical Distances to design notched metals against dynamic loading. *Materials and Design*, 69, pp. 197–212, 2015.

charts of Figure 2 clearly support the idea that, independently from the way \dot{Z} is defined, the selected experimental data can all be summarised by adopting simple power laws. This implies that both the σ_f vs. \dot{Z} relationship and the K_{Id} vs. \dot{Z} relationship can be rewritten as:

$$\sigma_f(\dot{Z}) = a_f \cdot \dot{Z}^{b_f} \quad (16)$$

$$K_{Id}(\dot{Z}) = \alpha \cdot \dot{Z}^\beta, \quad (17)$$

where a_f , b_f , α , and β are material constants to be determined by running appropriate experiments.

Remembering that, under static loading, σ_o is seen to be proportional to σ_{UTS} [20], the hypothesis can be formed that also the σ_o vs. \dot{Z} relationship can be expressed by adopting a power law, i.e.:

$$\sigma_o(\dot{Z}) = a_o \cdot \dot{Z}^{b_o}, \quad (18)$$

a_o and b_o being again material dependent constants.

According to Eq. (9), length scale parameter $L(\dot{Z})$ can now be rewritten in explicit form as:

$$L(\dot{Z}) = f_L(\dot{Z}) = \frac{1}{\pi} \left[\frac{K_{Id}(\dot{Z})}{\sigma_o(\dot{Z})} \right]^2 = \frac{1}{\pi} \left[\frac{\alpha \cdot \dot{Z}^\beta}{a_o \cdot \dot{Z}^{b_o}} \right]^2 = A \cdot \dot{Z}^B \quad (19)$$

In Eq. (19), A and B are material constants which have to be determined by post-processing appropriate experimental results. In particular, if $\sigma_o(\dot{Z})$ equals $\sigma_f(\dot{Z})$, then constants A and B can directly be estimated as soon as function $K_{Id}(\dot{Z})$, Eq. (17), is known from the experiments. On the contrary, for those situations in which $\sigma_o(\dot{Z})$ is different from $\sigma_f(\dot{Z})$,

Please, cite this paper as: Yin, T., Tyas, A., Plekhov, O., Terekhina, A., Susmel, L. A novel reformulation of the Theory of Critical Distances to design notched metals against dynamic loading. *Materials and Design*, 69, pp. 197–212, 2015.

such constants are suggested to be determined by adopting a strategy similar to the one summarised in Figure 1e. To conclude, it should be noted that, in the latter case, at least two sets of results generated by testing two different notches under two different values of \dot{Z} are required to determine constants A and B, the accuracy obviously increasing as the number of data used to calibrate the model increases.

5. Experimental details

In order to check the accuracy of the novel reformulation of the TCD formalised in the previous sections, three experimental trials were run in the testing laboratory of the Sheffield University at Harpur Hill, Buxton, UK and in the laboratory of the Institute of Continuous Media Mechanics UB RAS, Perm, Russia.

The experimental investigation performed at the University of Sheffield involved plain and notched cylindrical samples of Al6063-T5, such samples being tested under both quasi-static and dynamic tensile loading. In terms of conventional quasi-static mechanical properties, the investigated aluminium alloy had an ultimate tensile stress, σ_{UTS} , equal to 205 MPa, a yield stress, σ_y , of 145 MPa, an elastic modulus, E, of 68900 MPa, and a Poisson's ratio, ν , of 0.33. The geometries of the tested specimens are sketched in Figure 3. The plain samples had net diameter, d_n , equal to 5 mm and gross diameter, d_g , to 10 mm. The bluntly notched specimens had $d_n=5$ mm, $d_g=10$ mm, and notch root radius r_n equal to 4 mm, these resulting in a net stress concentration factor, K_t , of 1.25. The samples containing both the intermediate and the sharp stress concentrators had $d_n=5.2$ mm and $d_g=10$ mm, the notch root radius being equal to 1.38 mm ($K_t=1.69$) and to 0.38 mm ($K_t=2.93$), respectively.

Figure 4a shows the experimental arrangement which was used to generate the results summarised in Table 1. The specimens were mechanically attached to two purpose-built load cells by using nuts. The load cell at the distal end of the sample was fixed to a stiff end-stop

Please, cite this paper as: Yin, T., Tyas, A., Plekhov, O., Terekhina, A., Susmel, L. A novel reformulation of the Theory of Critical Distances to design notched metals against dynamic loading. *Materials and Design*, 69, pp. 197–212, 2015.

whilst the load cell at the proximal, or loaded end of the specimen was connected through transfer bars to a pneumatic loading system. The transfer bars were constrained to travel axially by being passed through PTFE-coated holes in the flanges of a steel column section, and the proximal load cell was sat on a PTFE slider. In this way, the loading system was free to translate under the applied load, subject only to the resistance of the specimen. The pneumatic pressure was generated by releasing pressurised bottled nitrogen into a barrel of a “gas gun” where it reacted against a close-fitting nylon sealing piston, to drive the a loading rod – cross-head – transfer bar system and hence apply a tensile load to the proximal load cell. Quasi-static loading was applied by slowly releasing the pneumatic pressure into the gas gun barrel. Dynamic loading was produced by releasing the pressurised nitrogen into a receiver vessel, separated from the gas gun barrel by a brass diaphragm which burst at a suitable pressure, causing a rapidly increasing load (typically of the order of 100-2000kN/s) to be applied to the specimen. The dynamic loading rate was changed by using different thickness bursting diaphragms and introducing a choke to limit the rate of gas flow from the receiver to the loading system.

The axial deformation and the cracking behaviour of the tested Al6063-T5 cylindrical samples were monitored by using a high-speed camera which was synchronised with the signals gathered from the loading cells. Camera Phantom V4.2 (8-bit image resolution, 2100 frames per second, recording at up to 90000 frames per second maximum) was used for Series 1 (S1 in Table 1), whereas camera Phantom V9.1 (14-bit image resolution, recording at up to 153846 fps) was employed for Series 2 (S2 in Table 1). By post-processing the video of any test it was possible to confirm that, in the force vs. time curve, a sharp decrease of the load signal corresponded to the formation of a visible crack. Accordingly, the maximum force recorded during each test was taken as the failure force, F_f , the corresponding instant being used to define the time to failure, T_f . The force vs. time diagram reported in Figure 4b shows the way the gathered signals were post-processed to determine F_f and T_f for test S1 T18 (see also Table 1). Here, the load is that recorded by the distal load cell, i.e. the load which was

Please, cite this paper as: Yin, T., Tyas, A., Plekhov, O., Terekhina, A., Susmel, L. A novel reformulation of the Theory of Critical Distances to design notched metals against dynamic loading. *Materials and Design*, 69, pp. 197–212, 2015.

transmitted through the specimen. It should be noted that the load does not immediately fall to zero on complete fracture of the specimen, due to inertia of the distal load cell which takes a few hundred microseconds to fully relax. The pictures extracted from the corresponding high-speed video and reported in the above diagram also confirm that the maximum force recorded during testing corresponded to the formation of a visible crack. The values for F_f and T_f determined according to the procedure briefly discussed above were then used to calculate the nominal loading rate, \dot{F} , as follows:

$$\dot{F} = \frac{F_f}{T_f} \quad (20)$$

Commercial software Cine viewer 2.14b was employed to post-process the high-speed videos in order to determine, for each test, the corresponding nominal strain, ε_{nom} , vs. time curve. For the notched samples, the gauge length was taken equal to the distance (measured along the axis) between the corners resulting from the intersection of the notch flanks with the cylindrical surface delimiting the gross volume of the specimens themselves. Accordingly, the gauge lengths, l_0 , for the sharp, intermediate and blunt notches were equal to 3.2 mm, 4.4 mm and 7.8 mm, respectively (see Figure 3). For each test, by post-processing the high-speed videos, the actual distance, l , between the two reference points was measured frame by frame throughout the test, the corresponding nominal strain being calculated as follows:

$$\varepsilon_{\text{nom}} = \frac{l - l_0}{l_0} \quad (21)$$

The diagram reported in Figure 4b shows an example of the nominal strain, ε_{nom} , vs. time curve determined according to the procedure described above. Finally, from any ε_{nom} vs. time

Please, cite this paper as: Yin, T., Tyas, A., Plekhov, O., Terekhina, A., Susmel, L. A novel reformulation of the Theory of Critical Distances to design notched metals against dynamic loading. *Materials and Design*, 69, pp. 197–212, 2015.

curve, the nominal failure strain, ε_f , was estimated at instant T_f , so that, the nominal strain rate, $\dot{\varepsilon}_{nom}$, could directly be calculated as follows:

$$\dot{\varepsilon}_{nom} = \frac{\varepsilon_f}{T_f} \quad (22)$$

Table 1 summarises the results generated by testing the samples of Al6063-T5 in terms of failure force, F_f , time to failure, T_f , nominal loading rate, \dot{F} , and nominal strain rate, $\dot{\varepsilon}_{nom}$.

The experimental investigation carried out at the Institute of Continuous Media Mechanics UB RAS involved three different metallic materials, i.e. titanium alloy Ti-6Al-4V having $\sigma_{UTS}=1031$ MPa, aluminium alloy AlMg6 having $\sigma_{UTS}=616$ MPa and an AlMn alloy having $\sigma_{UTS}=161$ MPa. The geometries of the tested samples are shown in Figure 5. In particular, independently from the sharpness of the notch, the specimens had gross diameter, d_g , equal to 9 mm and net diameter, d_n , to 7.6 mm. The three stress raisers had root radius equal to 2 mm, 1 mm, and 0.1 mm, resulting in a net stress concentration factor, K_t , equal to 1.67, 2.08, and 5.2 respectively.

The tensile tests under a nominal strain rate, $\dot{\varepsilon}_{nom}$, equal to 10^{-2} s^{-1} , 10^{-1} s^{-1} , and 10 s^{-1} were ran using a 100 kN servo-hydraulic machine Bi-00-100. The sharply notched samples instead were tested under $\dot{\varepsilon}_{nom} \approx 10^4 \text{ s}^{-1}$ by employing a classic Hopkinson-Kolsky split bar in the Nicholas's modification [56]. The experimental setup is a typical compression setup with incident and transmission bars. The threaded metallic specimens located on both the incident and transmission ends, while placing a metal collar over the specimen. The specimen and the metal collar had a snug fit on the incident and transmission side in order to bypass an initial compression wave. The initial compression wave was generated by an impact in the incident bar with a striker. The compression wave would ideally pass through

Please, cite this paper as: Yin, T., Tyas, A., Plekhov, O., Terekhina, A., Susmel, L. A novel reformulation of the Theory of Critical Distances to design notched metals against dynamic loading. *Materials and Design*, 69, pp. 197–212, 2015.

the metal collar and then reflect off the free end in tension. The tensile wave would then pull on the specimen.

The experimental setup in the Institute of Continuous Media Mechanics UB RAS includes two coaxial incident and transmitter bars with diameter of 25 mm and a 18-mm-caliber gas gun, which was used to accelerate a 200-mm-long projectile to a final velocity of 15-30 m/s. Two strain gauges fixed to the incident and transmitter bars were used to measure the stress waves in both bars. Following the classical consideration of elastic waves propagation in bars proposed by Kolsky and assuming the homogeneous stress-strain state into the sample we can derive the equation for calculation of stress, strain and strain rate of the specimen during the test [3]

$$\sigma_s(t) = \frac{ES}{S_b} \varepsilon_T(t), \quad \varepsilon_s(t) = -\frac{2C}{L} \int_0^t \varepsilon_R(t) dt, \quad \dot{\varepsilon}_s(t) = -\frac{2C}{L} \varepsilon_R(t) \quad (23)$$

where t is time, C the velocity of sound into the bars, L the initial specimen length, $\sigma_s(t)$ the stress in the specimen, $\varepsilon_s(t)$ and $\dot{\varepsilon}_s(t)$ the strain and strain rate, respectively, $\varepsilon_t(t)$ the strain wave into transmitter bar, and $\varepsilon_R(t)$ the strain wave reflected into incident bar. Parametric functions $\sigma_s(t)$, $\varepsilon_s(t)$ and $\dot{\varepsilon}_s(t)$ were used to directly calculate the stress-strain and strain rate-strain curves.

Finally, the results generated by testing plain and notched specimens of both Ti-6Al-4V and AlMn are summarised in Table 2 and 3, respectively, in terms of failure force, F_f , time to failure, T_f , nominal loading rate, \dot{F} , and nominal strain rate, $\dot{\varepsilon}_{nom}$.

6. Validation by experimental data

Please, cite this paper as: Yin, T., Tyas, A., Plekhov, O., Terekhina, A., Susmel, L. A novel reformulation of the Theory of Critical Distances to design notched metals against dynamic loading. *Materials and Design*, 69, pp. 197–212, 2015.

In order to check the accuracy of the proposed reformulation of the TCD in predicting the strength of the notched samples we tested under both quasi-static and dynamic loading, attention was initially focussed on the stress analysis problem. The relevant stress fields in the vicinity of the investigated stress concentrators were determined by using commercial FE software ANSYS®, where, independently from the considered loading/strain rate, the analysed materials were assumed to obey a linear-elastic constitutive law. The cylindrical samples were modelled by using axisymmetric bi-dimensional elements Plane42. For any notched geometry, the mapped mesh was gradually refined in the vicinity of the stress raiser apex until convergence occurred.

To use the TCD to re-analyse the results generated by testing the notched cylindrical samples of Al6063-T5, the initial assumption was made that the inherent strength could be taken equal to the corresponding parent material strength, that is:

$$\sigma_0(\dot{F}) = \sigma_f(\dot{F}) \text{ or } \sigma_0(\dot{\epsilon}_{\text{nom}}) = \sigma_f(\dot{\epsilon}_{\text{nom}}) \quad (24)$$

According to the plain results reported in Table 1, $\sigma_f(\dot{F})$ and $\sigma_f(\dot{\epsilon}_{\text{nom}})$ were expressed as follows:

$$\sigma_f(\dot{F}) = 209.9 \cdot \dot{F}^{0.0118} \quad [\text{MPa}] \quad (25)$$

$$\sigma_f(\dot{\epsilon}_{\text{nom}}) = 218.1 \cdot \dot{\epsilon}_{\text{nom}}^{0.0118} \quad [\text{MPa}] \quad (26)$$

The chart of Figure 6a shows the linear-elastic stress-distance curves plotted, under quasi-static loading (i.e., $\dot{F} \approx 0.15$ kN/s, $\dot{\epsilon}_{\text{nom}} \approx 0.01$ s⁻¹), in the incipient failure condition. This diagram fully confirms that, for this aluminium alloy, the inherent material strength could be taken equal to σ_{UTS} with little loss of accuracy. In particular, as shown in Figure 6a, the use of the material ultimate tensile strength ($\sigma_{\text{UTS}}=205$ MPa) together with a conventional best fit

Please, cite this paper as: Yin, T., Tyas, A., Plekhov, O., Terekhina, A., Susmel, L. A novel reformulation of the Theory of Critical Distances to design notched metals against dynamic loading. *Materials and Design*, 69, pp. 197–212, 2015.

procedure resulted in a value for the critical distance equal to 1.37 mm. The same chart shows also that the use of the TCD applied in the form of the PM with $\sigma_o = \sigma_{UTS} = 205$ MPa and $L = 1.37$ mm resulted in estimates falling within an error interval of $\pm 20\%$. Owing to the fact that this is the usual level of accuracy which is obtained when the TCD is used in other ambits of the structural integrity discipline [20, 57], hypothesis (24) was adopted to check the overall accuracy of TCD itself in estimating the strength of notched Al6063-T5 subjected to both quasi-static and dynamic loading.

After confirming the validity of assumption (24), the necessary critical distance value was then directly estimated through the results generated by testing both the plain and the sharply notched specimens (see Figure 3 and Table 1). In particular, functions $L(\dot{F})$ and $L(\dot{\epsilon}_{nom})$ were derived by post-processing the linear-elastic stress fields according to a procedure similar to the one summarised in Figure 1e, the only difference being that $\sigma_o(\dot{F}) = \sigma_f(\dot{F})$ and $\sigma_o(\dot{\epsilon}_{nom}) = \sigma_f(\dot{\epsilon}_{nom})$ were assumed to be known *a priori*. This *modus operandi* allowed us to obtain the following relationships – see Eq. (9):

$$L(\dot{F}) = 1.541 \cdot \dot{F}^{0.0368} \quad [\text{mm}] \quad (27)$$

$$L(\dot{\epsilon}_{nom}) = 1.695 \cdot \dot{\epsilon}_{nom}^{0.0343} \quad [\text{mm}] \quad (28)$$

By making use of power laws (27) and (28), the effective stress was then calculated, in the incipient failure condition, according to both the PM, Eq. (10), the LM, Eq. (11), and the AM, Eq. (12). The results of this final re-analysis are summarised in the two charts reported in Figures 6b and 6c, where the error is calculated as:

$$\text{Error} = \frac{\sigma_{\text{eff}}(\dot{Z}) - \sigma_o(\dot{Z})}{\sigma_o(\dot{Z})} \quad [\%] \quad (29)$$

Please, cite this paper as: Yin, T., Tyas, A., Plekhov, O., Terekhina, A., Susmel, L. A novel reformulation of the Theory of Critical Distances to design notched metals against dynamic loading. *Materials and Design*, 69, pp. 197–212, 2015.

According to the above definition, when the error is positive, estimates are conservative, whilst, when the error is negative, estimates are non-conservative.

The diagrams of Figures 6b and 6c make it evident that the novel formalisation of the TCD proposed in the present paper was highly accurate in predicting the dynamic strength of notched Al6063-T5, resulting in estimates falling within an error interval of $\pm 20\%$. This level of accuracy is considered to be acceptable, because, in general, it is not possible to distinguish between an error of $\pm 20\%$ and an error of 0% due to the problems which are usually encountered during testing as well as during the numerical analyses, the local material morphology playing a role of primary importance in defining the physiological level of scattering characterising the mechanical behaviour of engineering materials [20].

To check the accuracy of the TCD against the data generated by testing the samples of Ti-6Al-4V (see Table 2), also in this case, the initial hypothesis was formed that inherent strength could be taken equal to the corresponding plain material strength, the validity of such an hypothesis being checked *a posteriori* via the notch results. Accordingly, by using a conventional best fit procedure, functions $\sigma_o(\dot{\epsilon}_{nom})$ and $\sigma_o(\dot{F})$ were directly derived from the results generated by testing the un-notched specimens, i.e.:

$$\sigma_o(\dot{\epsilon}_{nom}) = \sigma_f(\dot{\epsilon}_{nom}) = 1080.8 \cdot \dot{\epsilon}_{nom}^{0.0094} \quad [\text{MPa}] \quad (30)$$

$$\sigma_o(\dot{F}) = \sigma_f(\dot{F}) = 1027 \cdot \dot{F}^{0.0129} \quad [\text{MPa}] \quad (31)$$

The linear-elastic stress fields plotted, in the incipient failure condition, in the chart of Figure 7a fully confirm the validity of the formed hypothesis. In more detail, the two stress-distance curves reported in the above graphs were determined by considering both the blunt ($K_t=1.67$) and the intermediate ($K_t=2.08$) stress raisers, the nominal failure force being calculated by averaging, for any notched geometry, the three results generated under $\dot{\epsilon}_{nom} = 0.01 \text{ s}^{-1}$ ($\dot{F} \approx 1.27 \text{ kN/s}$). This simple procedure resulted in a critical distance value

Please, cite this paper as: Yin, T., Tyas, A., Plekhov, O., Terekhina, A., Susmel, L. A novel reformulation of the Theory of Critical Distances to design notched metals against dynamic loading. *Materials and Design*, 69, pp. 197–212, 2015.

under quasi-static loading equal to 3.724 mm. The same strategy (Fig. 7b) was followed also to estimate the critical distance value under $\dot{\epsilon}_{\text{nom}} \approx 10^4 \text{ s}^{-1}$ ($\dot{F} \approx 2.4 \cdot 10^6 \text{ kN/s}$): the use of the liner-elastic stress-distance curve determined by averaging the two results generated by testing the sharply notched samples ($K_t=5.2$) together with the failure stress estimated according to Eq. (30) resulted in a critical distance value of 1.792 mm. Therefore, the two critical distance values estimated as described above allowed us to directly calculate constants A and B in Eq. (19), obtaining:

$$L(\dot{\epsilon}_{\text{nom}}) = 2.92 \cdot \dot{\epsilon}_{\text{nom}}^{-0.053} \quad [\text{mm}] \quad (32)$$

$$L(\dot{F}) = 3.77 \cdot \dot{F}^{-0.051} \quad [\text{mm}] \quad (33)$$

The error diagrams reported in Figures 7c and 7d prove that the proposed reformulation of the TCD was capable of accurately estimating also the strength of the notched specimens of Ti-6Al-4V, with the estimates falling within an error interval of $\pm 20\%$. It also interesting to point out that such a high level of accuracy was reached independently from the form in which the TCD was applied (i.e., in terms of either the PM, the LM, or the AM).

The results generated by testing the samples of the investigated AlMn alloy (Tab. 3) were re-analysed by adopting the same strategy as the one used to post-process the data obtained by testing the Ti-6Al-4V specimens. In particular, initially the inherent strength was assumed to be equal to the plain material failure stress, i.e.:

$$\sigma_0(\dot{\epsilon}_{\text{nom}}) = \sigma_f(\dot{\epsilon}_{\text{nom}}) = 182.5 \cdot \dot{\epsilon}_{\text{nom}}^{0.0363} \quad [\text{MPa}], \quad (34)$$

$$\sigma_0(\dot{F}) = \sigma_f(\dot{F}) = 167 \cdot \dot{F}^{0.0424} \quad [\text{MPa}] \quad (35)$$

where $\sigma_f(\dot{\epsilon}_{\text{nom}})$ and $\sigma_0(\dot{F})$ were determined through a conventional best fit procedure by considering the un-notched results listed in Table 3. The chart of Figure 8a reports the

Please, cite this paper as: Yin, T., Tyas, A., Plekhov, O., Terekhina, A., Susmel, L. A novel reformulation of the Theory of Critical Distances to design notched metals against dynamic loading. *Materials and Design*, 69, pp. 197–212, 2015.

critical distance value determined under $\dot{\epsilon}_{\text{nom}} = 0.01 \text{ s}^{-1}$ ($\dot{F} \approx 0.154 \text{ kN/s}$) by averaging the three results generated by testing the bluntly notched specimens ($K_t = 1.67$) - see Table 3. The chart of Figure 8b plots instead the linear-elastic stress distance curve determined, in the incipient failure condition, from the result obtained by testing a sharply notched specimen ($K_t = 5.2$) under $\dot{\epsilon}_{\text{nom}} \approx 10^4 \text{ s}^{-1}$ ($\dot{F} = 8.6 \cdot 10^4 \text{ kN/s}$). According to this chart, the corresponding critical distance value was estimated to be equal to 0.136 mm. The L values reported in Figure 8a and 8b were then used to estimate constants A and B in Eq. (19), obtaining:

$$L(\dot{\epsilon}_{\text{nom}}) = 0.841 \cdot \dot{\epsilon}_{\text{nom}}^{-0.198} \quad [\text{mm}] \quad (36)$$

$$L(\dot{F}) = 1.42 \cdot \dot{F}^{-0.206} \quad [\text{mm}] \quad (37)$$

The error diagrams reported in Figures 8c and 8d prove that the proposed reformulation of the TCD was highly accurate also in estimating the strength of the notched samples made of the investigated AlMn alloy, this holding true when the method was applied in terms of both strain (Fig. 8c) and loading rate (Fig. 8d).

The results generated by testing the samples of AlMn6 (Tab. 4) were post-processed by following the same strategy as the one adopted to re-analyse the data generated by testing the specimens made of both Ti-6Al-4V and AlMn alloy. By assuming that the inherent strength could be taken equal to the plain material failure stress, the following plain material calibration functions were obtained via a conventional best fit procedure:

$$\sigma_0(\dot{\epsilon}_{\text{nom}}) = \sigma_f(\dot{\epsilon}_{\text{nom}}) = 591.8 \cdot \dot{\epsilon}_{\text{nom}}^{-0.01} \quad [\text{MPa}], \quad (38)$$

$$\sigma_0(\dot{F}) = \sigma_f(\dot{F}) = 605.4 \cdot \dot{F}^{-0.01} \quad [\text{MPa}] \quad (39)$$

Please, cite this paper as: Yin, T., Tyas, A., Plekhov, O., Terekhina, A., Susmel, L. A novel reformulation of the Theory of Critical Distances to design notched metals against dynamic loading. *Materials and Design*, 69, pp. 197–212, 2015.

The negative exponents in Eqs (38) and (39) make it evident that this material was characterised by an inverse strain rate sensitivity, this representing a very interesting condition to further validate the accuracy of the proposed approach.

The chart of Figure 9a shows the L value determined under $\dot{\epsilon}_{\text{nom}} = 0.01 \text{ s}^{-1}$ ($\dot{F} \approx 0.094 \text{ kN/s}$) by averaging the three results obtained by testing the notched specimens having K_t equal to 2.08 - see Table 4. The diagram reported in Figure 9b shows instead the linear-elastic stress distance curves determined, in the incipient failure condition, by post-processing the result generated by testing, under $\dot{\epsilon}_{\text{nom}} = 10 \text{ s}^{-1}$ ($\dot{F} \approx 73.3 \text{ kN/s}$), the notched specimens having stress concentration factor, K_t , equal to both 1.67 and 2.08, the corresponding critical distance value being equal to 0.651 mm. The L values estimated under $\dot{\epsilon}_{\text{nom}} = 0.01 \text{ s}^{-1}$ as well as under $\dot{\epsilon}_{\text{nom}} = 10 \text{ s}^{-1}$ were then used to calculate the constants in Eq. (19), obtaining:

$$L(\dot{\epsilon}_{\text{nom}}) = 0.614 \cdot \dot{\epsilon}_{\text{nom}}^{0.0256} \quad [\text{mm}] \quad (40)$$

$$L(\dot{F}) = 0.614 \cdot \dot{F}^{0.0253} \quad [\text{mm}] \quad (41)$$

The error diagrams reported in Figures 9c and 9d make it clear that the proposed reformulation of the TCD was capable of accurately estimating the strength of the tested notched samples, even though aluminium AlMn6 was characterised by an inverse strain rate sensitivity.

To further investigate the reliability of the proposed reformulation of the TCD, the accuracy of our approach was also checked against the experimental results generated, back in the 60s, by Brisbane [51] by testing, under quasi-static and dynamic tensile loading, notched specimens of 301XH stainless steel, René-41 alloy, and Jet-1000 steel. The un-notched flat samples had width equal to 12.7 mm and gauge length equal to 50.8 mm. The V-notched flat specimens had a net width, w_n , of 15.24 mm and a gross width, w_g , of 25.4 mm. Four different values of the root radius, r_n , were investigated, i.e., $r_n = 0.05 \text{ mm}$ ($K_t = 14.7$), $r_n = 0.25$

Please, cite this paper as: Yin, T., Tyas, A., Plekhov, O., Terekhina, A., Susmel, L. A novel reformulation of the Theory of Critical Distances to design notched metals against dynamic loading. *Materials and Design*, 69, pp. 197–212, 2015.

mm ($K_t=6.8$), $r_n=1.27$ mm ($K_t=3.3$), and $r_n=4.95$ mm ($K_t=1.9$). The above samples were tested under the following values of the nominal displacement rate, $\dot{\Delta}$: 0.002 mm/s, 0.021 mm/s, 0.423 mm/s, and 3.387 mm/s. Table 4 summarises all the results generated by Brisbane [51], $\sigma_{n,f}$ being the nominal failure strength referred to the net area of the samples. It is worth observing here that the $\sigma_{n,f}$ values reported in Table 4 were supplied by Brisbane himself as the average from three different tests.

The linear-elastic stress fields needed to apply the TCD were calculated via bi-dimensional FE models done using commercial software ANSYS®, where the mesh in the vicinity of the stress raiser apices was gradually refined until convergence occurred.

The stress-distance curves plotted, in the incipient failure condition, in the charts of Figure 9 clearly prove that, for these three metallic materials, inherent strength $\sigma_o(\dot{\Delta})$ was larger than the corresponding failure strength, $\sigma_f(\dot{\Delta})$, this holding true independently from the considered value of the displacement rate. Accordingly, cases $\dot{\Delta}=0.002$ mm/s and $\dot{\Delta}=3.387$ mm/s were used to calibrate the constants not only in functions $L(\dot{\Delta})$ but also in functions $\sigma_o(\dot{\Delta})$, obtaining:

$$301XH \text{ Stainless steel} \Rightarrow \sigma_o(\dot{\Delta}) = 1889.8 \cdot \dot{\Delta}^{-0.027} \quad [\text{MPa}] \quad (42)$$

$$L(\dot{\Delta}) = 1.449 \cdot \dot{\Delta}^{0.0051} \quad [\text{mm}] - \quad (43)$$

$$\text{René-41 Alloy} \Rightarrow \sigma_o(\dot{\Delta}) = 2477.9 \cdot \dot{\Delta}^{0.012} \quad [\text{MPa}] - \quad (44)$$

$$L(\dot{\Delta}) = 0.529 \cdot \dot{\Delta}^{-0.084} \quad [\text{mm}] - \quad (45)$$

$$\text{Jet-1000 Steel} \Rightarrow \sigma_o(\dot{\Delta}) = 2503.3 \cdot \dot{\Delta}^{-0.005} \quad [\text{MPa}] - \quad (46)$$

$$L(\dot{\Delta}) = 1.468 \cdot \dot{\Delta}^{0.0188} \quad [\text{mm}] - \quad (47)$$

Please, cite this paper as: Yin, T., Tyas, A., Plekhov, O., Terekhina, A., Susmel, L. A novel reformulation of the Theory of Critical Distances to design notched metals against dynamic loading. *Materials and Design*, 69, pp. 197–212, 2015.

The error charts reported in Figure 10 show that the proposed approach was successful also in estimating the strength of the notched samples tested by Brisbane [51] under different values of the nominal displacement rate.

It is worth concluding the present section by observing that the accuracy obtained by using the proposed reformulation of the TCD is certainly promising, especially in light of the fact that it allows notched metals subjected to dynamic loading to be designed without the need for explicitly modelling the stress vs. strain non-linear behaviour of ductile metals. Accordingly, this novel reformulation of the TCD can be seen as a powerful engineering tool allowing practitioners to safely and accurately design notched metallic components/structures against dynamic loading by remarkably reducing the time and costs associated with the design process.

8. Conclusions

In the present paper a novel reformulation of the linear-elastic TCD suitable for designing notched metallic materials against dynamic loading is devised and validated by using a large number of experimental results. The most important conclusions can be summarised as follows:

- the proposed design methodology allows real components to be designed against dynamic loading by directly post-processing the relevant stress fields determined via conventional linear-elastic FE models. This implies that accurate estimates can be obtained without the need for explicitly modelling the mechanical response under dynamic loading of metallic materials;
- the proposed reformulation of the TCD is seen to be successful in estimating the strength of notched metallic materials subjected to dynamic loading;
- the performed validation exercise proves that the use of TCD in the form of either the PM, the LM, or the AM results in the same level of accuracy;

Please, cite this paper as: Yin, T., Tyas, A., Plekhov, O., Terekhina, A., Susmel, L. A novel reformulation of the Theory of Critical Distances to design notched metals against dynamic loading. *Materials and Design*, 69, pp. 197–212, 2015.

- the TCD is seen to be capable of estimates falling within an error interval of about $\pm 20\%$. Accordingly, when used in situations of practical interest, this approach is recommended to be used to design notched metallic materials against dynamic loading by adopting safety factors always larger than 1.2;
- more work needs to be done in this area to extend the use of the proposed design approach to those situations involving dynamic multiaxial loading.

ACKNOWLEDGEMENTS

The Perm Regional Government, Russia (Research project n. C-26/619) is acknowledged for supporting the present research investigation.

REFERENCES

- [1] Hopkinson B. A Method of Measuring the Pressure Produced in the Detonation of High Explosives or by the Impact of Bullets. *Proceedings of the Royal Society of London Series A, Containing Papers of a Mathematical and Physical Character*. 1914;89:411-3.
- [2] Davies R. A critical study of the Hopkinson pressure bar. *Philosophical Transactions of the Royal Society of London Series A Mathematical and Physical Sciences*. 1948:375-457.
- [3] Kolsky H. An Investigation of the Mechanical Properties of Materials at Very High Rates of Loading. *Proc. Phys. Soc. London, B62*, pp 676-687, 1949.
- [4] Lindholm US. Some experiments with the split Split hopkinson Hopkinson pressure bar. *Journal of the Mechanics and Physics of Solids*. 1964;12:317-35.
- [5] Lindholm US, Bessey RL, Smith GV. Effect of Strain Rate on Yield Strength, Tensile Strength, and Elongation of Three Aluminium Alloys. *J Mater*. 1971;6:119-33.
- [6] Oosterkamp LD, Ivankovic A, Venizelos G. High strain rate properties of selected aluminium alloys. *Materials Science and Engineering: A*. 2000;278:225-35.
- [7] Lee OS, Kim MS. Dynamic material property characterization by using split Hopkinson pressure bar (SHPB) technique. *Nuclear Engineering and Design*. 2003;226:119-25.
- [8] Zhang Xm, Li Hj, Li Hz, Gao H, Gao Zg, Liu Y, et al. Dynamic property evaluation of aluminum alloy 2519A by split Hopkinson pressure bar. *Transactions of Nonferrous Metals Society of China (English Edition)*. 2008;18:1-5.
- [9] Sakino K. Strain rate dependence of dynamic flow stress of 2017 aluminum alloy at very high strain rates. *International Journal of Modern Physics B*. 2008;22:1209-14.

Please, cite this paper as: Yin, T., Tyas, A., Plekhov, O., Terekhina, A., Susmel, L. A novel reformulation of the Theory of Critical Distances to design notched metals against dynamic loading. *Materials and Design*, 69, pp. 197–212, 2015.

[10] Wiesner CS, MacGillivray H. Loading Rate Effects on Tensile Properties and Fracture Toughness of Steel. 1999 TAGSI Seminar, Cambridge, IoM Publication. 1999:149.

[11] Yokoyama T, Kishida K. A novel impact three-point bend test method for determining dynamic fracture-initiation toughness. *Experimental Mechanics*. 1989;29:188-94.

[12] Li C.-J. Effects of temperature and loading rate on fracture toughness of structural steels. *Materials & Design* 21, Issue 1, 19 December 1999, pp. 27-30

[13] Neuber H. Theorie der technischen Formzahl. *Forsch Ing-Wes*. 1936;7:271-4.

[14] Peterson R. Notch sensitivity. *Metal fatigue*. 1959:293-306.

[15] Novozhilov VV. On a necessary and sufficient criterion for brittle strength: *PMM* vol. 33, (2), 1969, pp. 212–222. *Journal of Applied Mathematics and Mechanics*. 1969;33:201-10.

[16] Novozhilov VV. On the foundations of a theory of equilibrium cracks in elastic solids: *PMM* vol. 33, (5), 1969, pp. 797–812. *Journal of Applied Mathematics and Mechanics*. 1969;33:777-90.

[17] Whitney JM, Nuismer RJ. Stress Fracture Criteria for Laminated Composites Containing Stress Concentrations. *Journal of Composite Materials*. 1974;8:253-65.

[18] Tanaka K. Engineering formulae for fatigue strength reduction due to crack-like notches. *International Journal of Fracture*. 1983;22:R39-R46.

[19] Taylor D. Geometrical effects in fatigue: a unifying theoretical model. *International Journal of Fatigue*. 1999;21:413-20.

[20] Taylor D. *The Theory of Critical Distances: A New Perspective in Fracture Mechanics*: Elsevier Science Limited; 2007.

[21] Susmel L, Taylor D. Two methods for predicting the multiaxial fatigue limits of sharp notches. *Fatigue & Fracture of Engineering Materials & Structures*. 2003;26:821-33.

[22] Susmel L. A unifying approach to estimate the high-cycle fatigue strength of notched components subjected to both uniaxial and multiaxial cyclic loadings. *Fatigue & Fracture of Engineering Materials & Structures*. 2004;27:391-411.

[23] Susmel L, Taylor D. A simplified approach to apply the theory of critical distances to notched components under torsional fatigue loading. *International Journal of Fatigue*. 2006;28:417-30.

[24] Susmel L, Taylor D. On the use of the Theory of Critical Distances to predict static failures in ductile metallic materials containing different geometrical features. *Engineering Fracture Mechanics*. 2008;75:4410-21.

[25] Susmel L, Taylor D. The Theory of Critical Distances to estimate the static strength of notched samples of Al6082 loaded in combined tension and torsion. Part II: Multiaxial static assessment. *Engineering Fracture Mechanics*. 2010;77:470-8.

[26] Madrazo V, Cicero S, Carrascal IA. On the Point Method and the Line Method notch effect predictions in Al7075-T651. *Engineering Fracture Mechanics*. 2012;79:363-79.

Please, cite this paper as: Yin, T., Tyas, A., Plekhov, O., Terekhina, A., Susmel, L. A novel reformulation of the Theory of Critical Distances to design notched metals against dynamic loading. *Materials and Design*, 69, pp. 197–212, 2015.

[27] Cicero S, Madrazo V, Carrascal I. Analysis of notch effect in PMMA using the Theory of Critical Distances. *Engineering Fracture Mechanics*. 2012;86:56-72.

[28] Cicero S, Madrazo V, García T, Cuervo J, Ruiz E. On the notch effect in load bearing capacity, apparent fracture toughness and fracture mechanisms of polymer PMMA, aluminium alloy Al7075-T651 and structural steels S275JR and S355J2. *Engineering Failure Analysis*. 2013;29:108-21.

[29] Susmel L, Taylor D. The Theory of Critical Distances to estimate the static strength of notched samples of Al6082 loaded in combined tension and torsion. Part I: Material cracking behaviour. *Engineering Fracture Mechanics*. 2010;77:452-69.

[30] Taylor D. Predicting the fracture strength of ceramic materials using the theory of critical distances. *Eng. Frac. Mech*. 2004;71:2407-2416.

[31] Taylor D, Cornetti P, Pugno N. The fracture mechanics of finite crack extension. *Eng. Frac. Mech*. 2005;72:1021-1038.

[32] Susmel L., Taylor D., The Theory of Critical Distances as an alternative experimental strategy for the determination of K_{Ic} and ΔK_{th} . *Engineering Fracture Mechanics*, 77, pp. 1492–1501, 2010.

[33] Morozov, N. F., Petrov, Y. V., Dynamic fracture toughness in crack growth initiation problems. *Izv. AN SSSR MTT (Solid Mechanics)* 6, 108-11, 1990 (in Russian)

[34] Petrov, Y. V., Morozov, N. F., Smirnov, V. I., Structural macromechanics approach in dynamics of fracture. *Fatigue Fract Engng Mater Struct* 26, 363–372, 2003.

[35] Couque, H., Asaro, R. J., Duffy, J., Lee, S. H., Correlations of microstructure with dynamic and quasi-static fracture in a plain carbon steel. *Metall. Trans. A*, 19, pp. 2179–2206.

[36] Godse, R., Ravichandran, G., and Clifton, R. J., Micromechanisms of Dynamic Crack Propagation in an AISI-4340 Steel, *Mater. Sci. Eng.*, A112, 79-88, 1989.

[37] Drar, H., Bergmark, A., Load rate influence on the fracture morphology of a ductile steel. *Engineering Fracture Mechanics* 46 2, 225–233, 1993.

[38] Venkert, A., Guduru, P. R., Ravichandran, G. Effect of Loading Rate on Fracture Morphology in a High Strength Ductile Steel. *Journal of Engineering Materials and Technology (Trans. ASME)* 123, 261-267, 2001.

[39] Naimark O.B. Defect induced instabilities in condensed media, *JETP Letters*, 67 (9), 751-758, 1998.

[40] Plekhov O. A. Modeling of stochastic properties of fast cracks in quasi-brittle materials. *Computational Materials Science* 28/3-4, 462-468, 2003.

[41] Huang Y., Young B., The art of coupon tests. *Journal of Constructional Steel Research* 96 (2014) 159–175.

[42] Liang, H., Pan, F., Wang, J. and Yang, J. (2013). Tensile and Compressive Properties of Mg-3Al-2Zn-2Y Alloy at Different Strain Rates. *Journal of Materials Engineering and Performance*, Volume 22, Issue 9, pp 2681-2690.

Please, cite this paper as: Yin, T., Tyas, A., Plekhov, O., Terekhina, A., Susmel, L. A novel reformulation of the Theory of Critical Distances to design notched metals against dynamic loading. *Materials and Design*, 69, pp. 197–212, 2015.

[43] Grassel, O., Kruger, L., Frommeyer, G., Meyer, L.W. (2009). Predicting of mechanical properties of Fe–Mn–(Al, Si) TRIP/TWIP steels using neural network modeling. *Computational Materials Science*, Volume 45, Issue 4, June 2009, Pages 959–965.

[44] Lin, Y., Wu, S. and Kao, F. et al. (2011). Microtwin formation in the α phase of duplex titanium alloys affected by strain rate. *Materials Science and Engineering: A*, Volume 528, Issue 6, Pages 2271-2276.

[45] El-Gamal, S., Mohammed, Gh. (2014). Effects of γ -irradiation and strain rate on the tensile and the electrical properties of Al-4043 alloy. *Radiation Physics and Chemistry*, Volume 99, June 2014, Pages 68-73.

[46] Boyce, B.L. and Dilmore, M.F. (2009). The dynamic tensile behavior of tough, ultrahigh-strength steels at strain-rates from 0.0002 s⁻¹ to 200 s⁻¹. *International Journal of Impact Engineering*, Volume 36, Issue 2, February 2009, Pages 263-271.

[47] Børvik, T., Hopperstad, O.S., Berstad, T. and Langseth, M. (2001). A computational model of viscoplasticity and ductile damage for impact and penetration. *European Journal of Mechanics - A/Solids*, Volume 20, Issue 5, September–October 2001, Pages 685-712.

[48] Solomos, G., Albertini, C., Labibes, K., Pizzinato, V., Viaccoz, B. (2004). Strain rate effects in nuclear steels at room and higher temperatures. *Nuclear Engineering and Design*, Volume 229, Issues 2–3, April 2004, Pages 139-149.

[49] Xu, S., Tyson, W.R., Bouchard, R. and Gertsman, V.Y. (2009). Effects of Strain Rate and Temperature on Tensile Flow Behavior and Energy Absorption of Extruded Magnesium AM30 Alloy. *Journal of Materials Engineering and Performance*, November 2009, Volume 18, Issue 8, pp 1091-1101.

[50] Cao, R., Lei, M.X., Chen, J.H., Zhang, J. (2007). Effects of loading rate on damage and fracture behavior of TiAl alloys. *Materials Science and Engineering: A*, Volume 465, Issues 1–2, 15 September 2007, Pages 183-193.

[51] Brisbane, A. W., The investigation of the effects of loading rate and stress concentration factors on the notch properties of three sheet alloy at subzero temperatures. Technical Documentary Report No. ASD-TDR-62-930, Project No. 7351, Task No. 735106, Directorate of Material and Processes, Wright-Patterson Air Force Base, Ohio, USA, March 1963.

[52] Li C.-J., Effects of temperature and loading rate on fracture toughness of structural steels, *Materials and Design* 21, 2000, pp. 27-30.

[53] Sun, Z. M., Kobayashi, T., Fukumasu, H., Yamamoto, I. and K. Shibue (1998). Tensile Properties and Fracture Toughness of a Ti-45Al-1.6Mn Alloy at Loading Velocities of up to 12 m/s. *Metallurgical and Materials Transactions A*, January 1998, Volume 29, Issue 1, pp 263-277.

[54] Priest A. M., Influence of strain rate and temperature on the fracture and tensile properties of several metallic materials. In: *Proceeding of Conference on Dynamic Fracture Toughness*, Paper 10, The Welding Institute, 1977.

[55] Shapiro, J., Sharpe, W. and Tregoning, R. (1992). Dynamic Crack-Tip Opening Displacement (CTOD) Measurements with Application to Fracture Toughness Testing. *STP1130*, January 1992, pp 118-133.

Please, cite this paper as: Yin, T., Tyas, A., Plekhov, O., Terekhina, A., Susmel, L. A novel reformulation of the Theory of Critical Distances to design notched metals against dynamic loading. *Materials and Design*, 69, pp. 197–212, 2015.

[56] Nicholas T. Tensile Testing of Materials at High Rates of Strain, *Exp. Mech.* 21, 177-188, 1981.

[57] Susmel L. *Multiaxial notch fatigue: from nominal to local stress–strain quantities*. Cambridge (UK): Woodhead & CRC; 2009.

List of Captions

- Table 1.** Summary of the experimental results generated by testing plain and notched cylindrical samples of Al6063-T5.
- Table 2.** Summary of the experimental results generated by testing plain and notched cylindrical samples of Ti-6Al-4V.
- Table 3.** Summary of the experimental results generated by testing plain and notched cylindrical samples of AlMn alloy.
- Table 4.** Summary of the experimental results generated by testing plain and notched cylindrical samples of AlMg6.
- Table 5.** Summary of the results generated by Brisbane [51] by testing plain and V-notched flat samples of 301XH Stainless steel, René-41 Alloy, and Jet-1000 Steel.
- Figure 1.** Definition of the local systems of coordinates (a). Effective stress, σ_{eff} , calculated according to the Point Method (b), Line Method (c), and Area Method (d). Determination of length scale parameter L and inherent strength σ_0 through experimental results generated by testing notches of different sharpness (e).
- Figure 2.** σ_f vs. \dot{Z} and K_{Id} vs. \dot{Z} relationships determined by post-processing experimental data taken from the technical literature.
- Figure 3.** Geometries of the samples of Al6063-T5 tested at the University of Sheffield (dimensions in millimetre).
- Figure 4.** Experimental rig used to test the notched cylindrical samples of Al6063-T5 (a); force vs. time and nominal strain vs. time curve for test S1 T18 (b).
- Figure 5.** Geometries of the samples tested in the laboratory of the Institute of Continuous Media Mechanics UB RAS, Perm, Russia (dimensions in millimetres).
- Figure 6.** Local linear-elastic stress fields, in the incipient failure condition, under quasi-static loading ($\dot{F} \approx 0.15$ kN/s, $\dot{\epsilon}_{\text{nom}} \approx 0.01$ 1/s) for notched Al6063-T5 (a); accuracy of the TCD applied in terms of both loading rate (b) and nominal strain rate (c) in predicting the strength of notched Al6063-T5.
- Figure 7.** Local linear-elastic stress fields, in the incipient failure condition, under $\dot{\epsilon}_{\text{nom}} = 0.01$ 1/s (a) and $\dot{\epsilon}_{\text{nom}} = 10^4$ 1/s (b) for notched Ti-6Al-4V; accuracy of the TCD in predicting the strength of notched Ti-6Al-4V (c, d).
- Figure 8.** Local linear-elastic stress fields, in the incipient failure condition, under $\dot{\epsilon}_{\text{nom}} = 0.01$ 1/s (a) and $\dot{\epsilon}_{\text{nom}} = 10^4$ 1/s (b) for notched AlMn alloy; accuracy of the TCD in predicting the strength of notched AlMn alloy (c, d).
- Figure 9.** Local linear-elastic stress fields, in the incipient failure condition, under $\dot{\epsilon}_{\text{nom}} = 0.01$ 1/s (a) and $\dot{\epsilon}_{\text{nom}} = 10^4$ 1/s (b) for notched AlMg6; accuracy of the TCD in predicting the strength of notched AlMg6 alloy (c, d).
- Figure 10.** Local linear-elastic stress fields, in the incipient failure condition, under $\dot{\Delta} = 0.002$ mm/s and $\dot{\Delta} = 3.387$ mm/s for notched metallic materials 301XH, René-41, and Jet-1000 (data taken from Ref. [51]).
- Figure 11.** Accuracy of the TCD in predicting the strength of notched metallic materials 301XH, René-41, and Jet-1000 (data taken from Ref. [51]).

Tables

Code	d_g [mm]	d_n [mm]	r_n [mm]	K_t	F_f [kN]	T_f [s]	\dot{F} [kN/s]	$\dot{\epsilon}_{nom}$ [1/s]
S1 T1	10	5	Plain	1.00	3.8	4.1	0.9268	0.02
S1 T2	10	5	Plain	1.00	4.8	0.08	60.00	1.3
S1 T3	10	5	Plain	1.00	4.1	35	0.1171	0.007
S1 T5	10	5	Plain	1.00	4.6	0.05	92.00	3.5
S1 T6	10	5	Plain	1.00	4	0.02	200.0	8.2
S1 T7	10	5	Plain	1.00	4.4	0.006	733.3	19.8
S1 T8	10	5	Plain	1.00	4.5	0.005	900.0	21.7
S1 T11	10	5	Plain	1.00	4.1	0.004	1600	30.66
S1 T12	10	5	Plain	1.00	4.7	0.01	470.0	11.33
S1 T9	10	5.2	0.38	2.93	5.4	22	0.2455	0.013
S1 T10	10	5.2	0.38	2.93	6.7	0.004	1675	125
S2 T1	10	5.2	0.38	2.93	6.8	0.007	971.4	52.15
S2 T2	10	5.2	0.38	2.93	6.7	0.007	957.1	32.35
S1 T17	10	5.21	1.38	1.69	4.6	29	0.1586	0.01
S1 T18	10	5.21	1.38	1.69	6.2	0.003	2066.7	89.29
S2 T5	10	5.21	1.38	1.69	5.3	21	0.2524	0.01
S2 T6	10	5.21	1.38	1.69	5.1	16	0.3188	0.019
S2 T7	10	5.21	1.38	1.69	6.7	0.007	957.1	61.59
S2 T9	10	5.21	1.38	1.69	6.2	0.009	688.9	49.42
S2 T10	10	5.21	1.38	1.69	6.9	0.007	985.7	56.43
S2 T11	10	5.21	1.38	1.69	4.9	11	0.4455	0.03
S2 T12	10	5.21	1.38	1.69	5.2	16	0.3250	0.017
S2 T13	10	5.21	1.38	1.69	6	0.007	857.1	48.17
S2 T14	10	5.21	1.38	1.69	5.9	0.009	655.6	42.62
S1 T15	10	5	4.00	1.25	3.7	30	0.1233	0.01
S1 T16	10	5	4.00	1.25	3.5	23	0.1522	0.01

Table 1. Summary of the experimental results generated by testing plain and notched cylindrical samples of Al6063-T5.

Code	d_g [mm]	d_n [mm]	r_n [mm]	K_t	F_f [kN]	T_f [s]	\dot{F} [kN/s]	$\dot{\epsilon}_{nom}$ [1/s]
Ti-P1	9	7.6	plain	1.00	65.5	32.86	1.994	0.01
Ti-P2	9	7.6	plain	1.00	65.6	30.55	2.147	0.01
Ti-P3	9	7.6	plain	1.00	65.7	38.42	1.710	0.01
Ti-P4	9	7.6	plain	1.00	67.3	3.25	20.71	0.1
Ti-P5	9	7.6	plain	1.00	68.2	3.23	21.10	0.1
Ti-P6	9	7.6	plain	1.00	67.6	3.13	21.60	0.1
Ti-P7	9	7.6	plain	1.00	70.4	0.15	469.5	10
Ti-P8	9	7.6	plain	1.00	70.6	0.26	271.6	10
Ti-P9	9	7.6	plain	1.00	69.3	0.24	288.9	10
Ti-B1	9	7.6	2.0	1.67	56.3	52.77	1.067	0.01
Ti-B2	9	7.6	2.0	1.67	55.9	43.91	1.274	0.01
Ti-B3	9	7.6	2.0	1.67	57.1	43.09	1.326	0.01
Ti-B4	9	7.6	2.0	1.67	58.1	5.12	11.35	0.1
Ti-B5	9	7.6	2.0	1.67	58.2	5.19	11.22	0.1
Ti-B6	9	7.6	2.0	1.67	56.8	4.93	11.52	0.1
Ti-B7	9	7.6	2.0	1.67	61.9	0.38	162.9	10
Ti-B8	9	7.6	2.0	1.67	61.7	0.19	324.5	10
Ti-B9	9	7.6	2.0	1.67	61.9	0.21	294.6	10
Ti-I1	9	7.6	1.0	2.08	59.0	45.96	1.284	0.01
Ti-I2	9	7.6	1.0	2.08	58.8	43.31	1.358	0.01
Ti-I3	9	7.6	1.0	2.08	60.2	46.92	1.282	0.01
Ti-I4	9	7.6	1.0	2.08	59.8	4.7	12.72	0.1
Ti-I5	9	7.6	1.0	2.08	60.2	5.06	11.91	0.1
Ti-I6	9	7.6	1.0	2.08	60.6	5.3	11.43	0.1
Ti-I7	9	7.6	1.0	2.08	63.7	0.21	303.4	10
Ti-I8	9	7.6	1.0	2.08	63.5	0.23	276.0	10
Ti-I9	9	7.6	1.0	2.08	63.8	0.21	304.0	10
Ti-S1	9	7.6	0.1	5.2	56.3	$2.6 \cdot 10^{-5}$	$2.2 \cdot 10^6$	$\approx 10^4$
Ti-S2	9	7.6	0.1	5.2	71.2	$2.7 \cdot 10^{-5}$	$2.6 \cdot 10^6$	$\approx 10^4$

Table 2. Summary of the experimental results generated by testing plain and notched cylindrical samples of Ti-6Al-4V.

Code	d_g [mm]	d_n [mm]	r_n [mm]	K_t	F_f [kN]	T_f [s]	\dot{F} [kN/s]	$\dot{\epsilon}_{nom}$ [1/s]
AlMn-P1	9	7.6	plain	1.0	10.3	58.52	0.1752	0.01
AlMn-P2	9	7.6	plain	1.0	10.2	87.78	0.1167	0.01
AlMn-P3	9	7.6	plain	1.0	10.2	60.35	0.1690	0.01
AlMn-P4	9	7.6	plain	1.0	10.5	4.12	2.560	0.1
AlMnP5	9	7.6	plain	1.0	9.2	3.8	2.416	0.1
AlMn-P6	9	7.6	plain	1.0	10.5	4.25	2.462	0.1
AlMn-P7	9	7.6	plain	1.0	19.6	0.18	109.1	10
AlMn-P8	9	7.6	plain	1.0	10.5	0.18	58.07	10
AlMn-P9	9	7.6	plain	1.0	10.4	0.16	65.10	10
AlMn-B1	9	7.6	2.0	1.67	8.2	44.79	0.1840	0.01
AlMn-B2	9	7.6	2.0	1.67	8.1	57.64	0.1412	0.01
AlMn-B3	9	7.6	2.0	1.67	7.4	54.75	0.1354	0.01
AlMn-B4	9	7.6	2.0	1.67	8.4	4.11	2.054	0.1
AlMn-B5	9	7.6	2.0	1.67	8.3	4.49	1.856	0.1
AlMn-B6	9	7.6	2.0	1.67	8.4	4.5	1.857	0.1
AlMn-B7	9	7.6	2.0	1.67	8.0	0.21	38.29	10
AlMn-B8	9	7.6	2.0	1.67	7.1	0.2	35.72	10
AlMn-B9	9	7.6	2.0	1.67	8.9	0.18	49.47	10
AlMn-S1	9	7.6	0.1	5.2	5.0	$5.8 \cdot 10^{-5}$	$8.6 \cdot 10^4$	$\approx 10^4$

Table 3. Summary of the experimental results generated by testing plain and notched cylindrical samples of AlMn alloy.

Code	d_g [mm]	d_n [mm]	r_n [mm]	K_t	F_f [kN]	T_f [s]	[kN/s]	[1/s]
AlMg6-P1	9	7.6	plain	1.0	27.9	280.15	0.0996	0.01
AlMg6-P2	9	7.6	plain	1.0	27.8	269.69	0.1031	0.01
AlMg6-P3	9	7.6	plain	1.0	28.2	286.83	0.0982	0.01
AlMg6-P4	9	7.6	plain	1.0	27.7	26.22	1.058	0.1
AlMg6-P5	9	7.6	plain	1.0	27.7	26.98	1.027	0.1
AlMg6-P6	9	7.6	plain	1.0	27.7	26.064	1.061	0.1
AlMg6-P7	9	7.6	plain	1.0	26.2	0.31	84.5	10
AlMg6-P8	9	7.6	plain	1.0	26.2	0.29	90.41	10
AlMg6-P9	9	7.6	plain	1.0	26.1	0.32	81.47	10
AlMg6-B1	9	7.6	2.0	1.67	21.4	245.18	0.0874	0.01
AlMg6-B2	9	7.6	2.0	1.67	21.8	255.7	0.0853	0.01
AlMg6-B3	9	7.6	2.0	1.67	21.9	248.2	0.0882	0.01
AlMg6-B4	9	7.6	2.0	1.67	21.7	26.24	0.826	0.1
AlMg6-B5	9	7.6	2.0	1.67	21.6	25.08	0.860	0.1
AlMg6-B6	9	7.6	2.0	1.67	21.5	26.29	0.818	0.1
AlMg6-B7	9	7.6	2.0	1.67	20.9	0.32	65.31	10
AlMg6-B8	9	7.6	2.0	1.67	21.4	0.32	66.84	10
AlMg6-B9	9	7.6	2.0	1.67	21.0	0.32	65.72	10
AlMg6-I1	9	7.6	1.0	2.08	21.7	228.54	0.09	0.01
AlMg6-I2	9	7.6	1.0	2.08	21.4	220.5	0.10	0.01
AlMg6-I3	9	7.6	1.0	2.08	21.3	224.77	0.09	0.01
AlMg6-I4	9	7.6	1.0	2.08	21.5	24.46	0.88	0.1
AlMg6-I5	9	7.6	1.0	2.08	21.3	22.88	0.93	0.1
AlMg6-I6	9	7.6	1.0	2.08	21.2	22.82	0.93	0.1
AlMg6-I7	9	7.6	1.0	2.08	21.1	0.3	70.30	10
AlMg6-I8	9	7.6	1.0	2.08	21.1	0.3	70.37	10
AlMg6-I9	9	7.6	1.0	2.08	21.5	0.33	65.091	10

Table 4. Summary of the experimental results generated by testing plain and notched cylindrical samples of AlMg6.

w_g	w_n	r_n	K_t	$\dot{\Delta}$	301XH	René-41	Jet-10 0 0
					$\sigma_{n,f}$	$\sigma_{n,f}$	$\sigma_{n,f}$
[mm]	[mm]	[mm]		[mm/s]	[MPa]	[MPa]	[MPa]
12.7	12.7	plain	1.0	0.002	1392.1	1379.0	1410.7
12.7	12.7	plain	1.0	0.021	1390.7	1347.2	1407.2
12.7	12.7	plain	1.0	0.423	1393.4	1363.8	1413.4
12.7	12.7	plain	1.0	3.387	1405.2	1368.6	1508.6
25.4	15.24	0.05	14.7	0.002	1481.0	1132.8	1732.0
25.4	15.24	0.05	14.7	0.021	1529.9	1157.6	1676.1
25.4	15.24	0.05	14.7	0.423	1522.4	1194.2	1692.7
25.4	15.24	0.05	14.7	3.387	1212.8	909.4	1737.5
25.4	15.24	0.25	6.8	0.002	1522.4	1254.8	1709.9
25.4	15.24	0.25	6.8	0.021	1510.0	1300.4	1732.0
25.4	15.24	0.25	6.8	0.423	1521.7	1291.4	1737.5
25.4	15.24	0.25	6.8	3.387	1270.0	992.8	1748.5
25.4	15.24	1.27	3.3	0.002	1532.7	1373.4	1816.1
25.4	15.24	1.27	3.3	0.021	1516.8	1363.8	1799.5
25.4	15.24	1.27	3.3	0.423	1482.4	1421.0	1760.2
25.4	15.24	1.27	3.3	3.387	1263.1	1174.2	1782.3
25.4	15.24	4.95	1.9	0.002	1521.7	1442.4	1737.5
25.4	15.24	4.95	1.9	0.021	1516.8	1450.7	1743.0
25.4	15.24	4.95	1.9	0.423	1503.1	1443.8	1760.2
25.4	15.24	4.95	1.9	3.387	1256.9	1462.4	1720.9

Table 4. Summary of the results generated by Brisbane [51] by testing plain and V-notched flat samples of 301XH Stainless steel, René-41 Alloy, and Jet-1000 Steel.

Figures

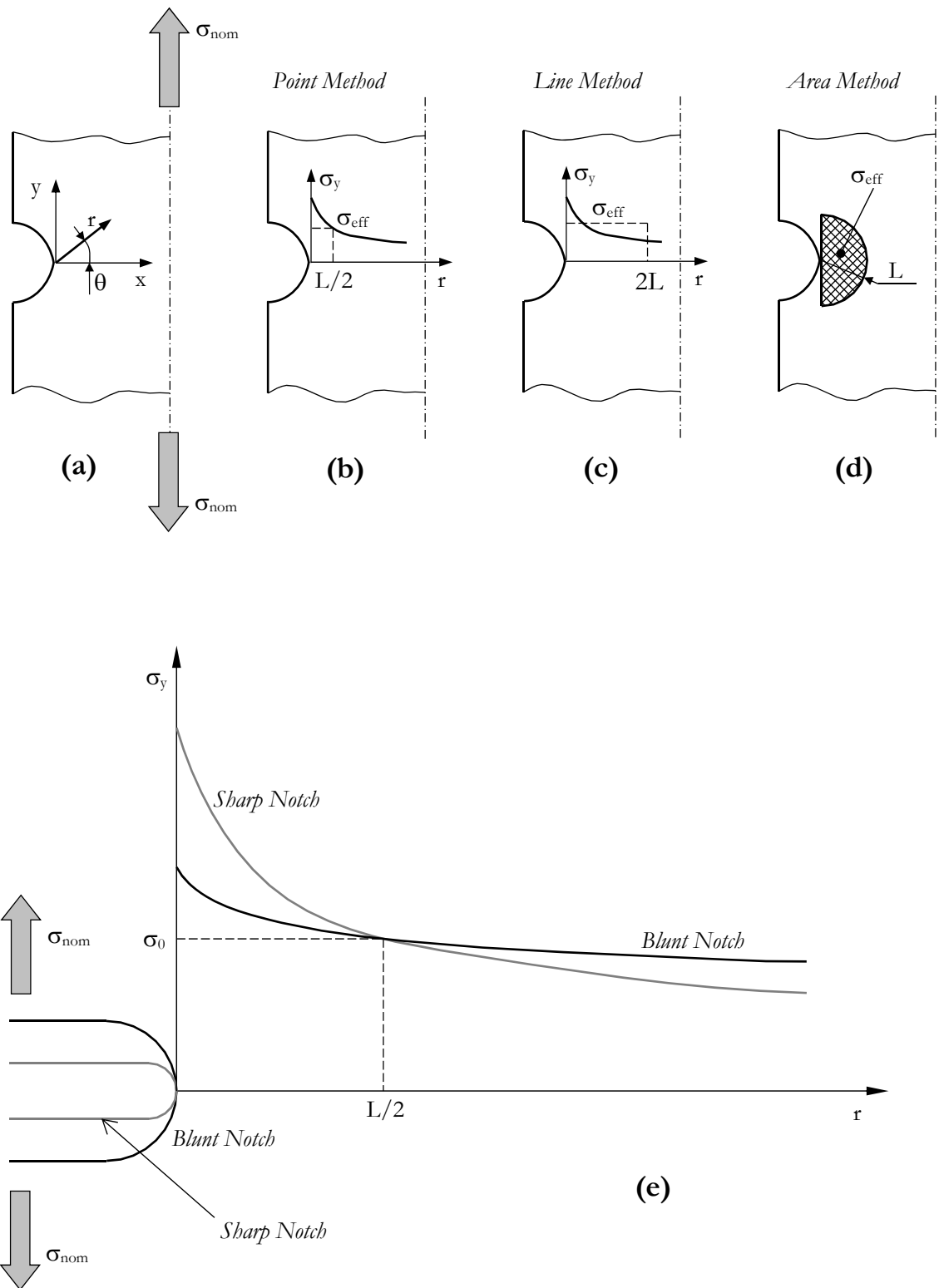


Figure 1. Definition of the local systems of coordinates (a). Effective stress, σ_{eff} , calculated according to the Point Method (b), Line Method (c), and Area Method (d). Determination of length scale parameter L and inherent strength σ_0 through experimental results generated by testing notches of different sharpness (e).

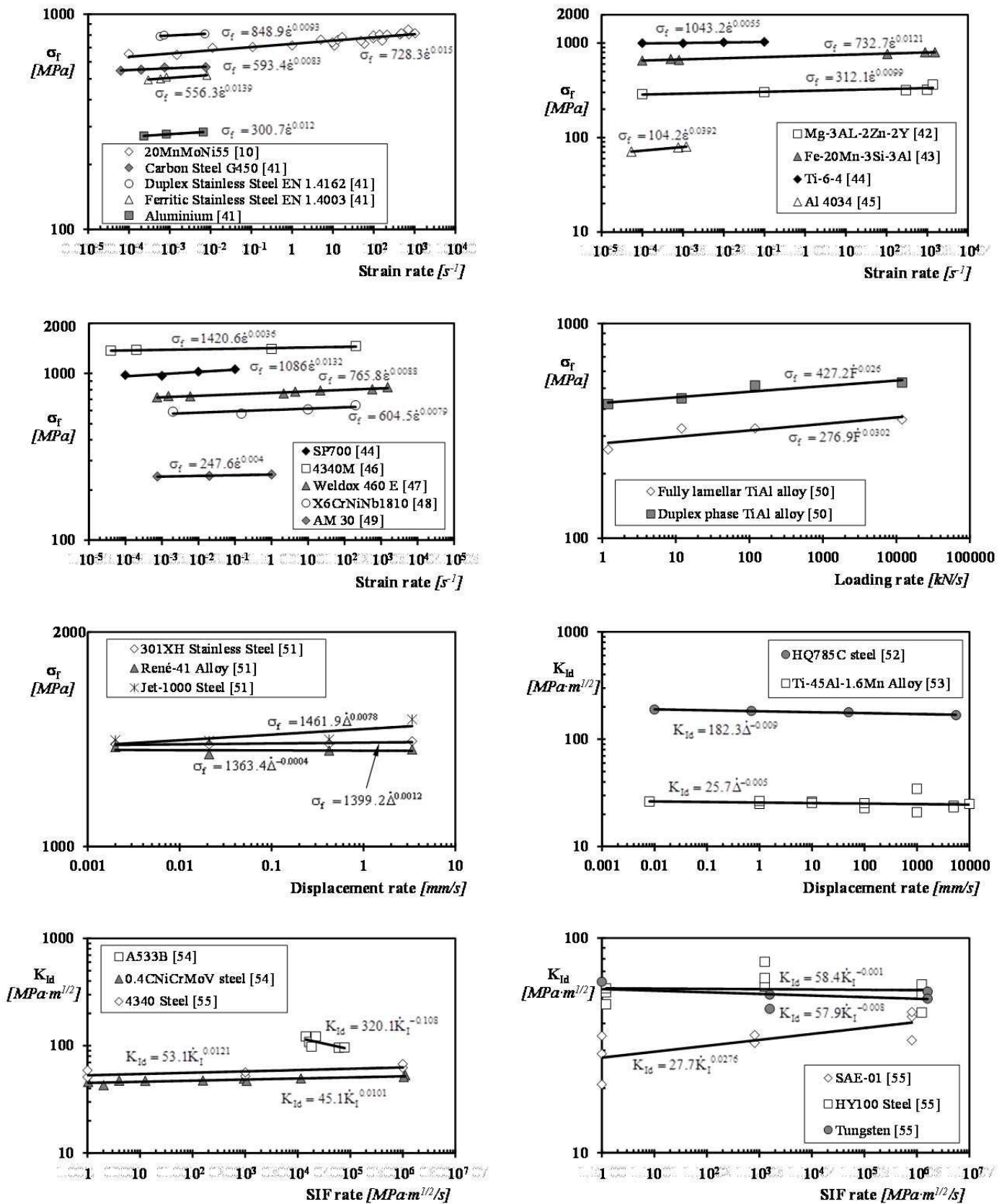


Figure 2. σ_f vs. \dot{Z} and K_{Id} vs. \dot{Z} relationships determined by post-processing experimental data taken from the technical literature.

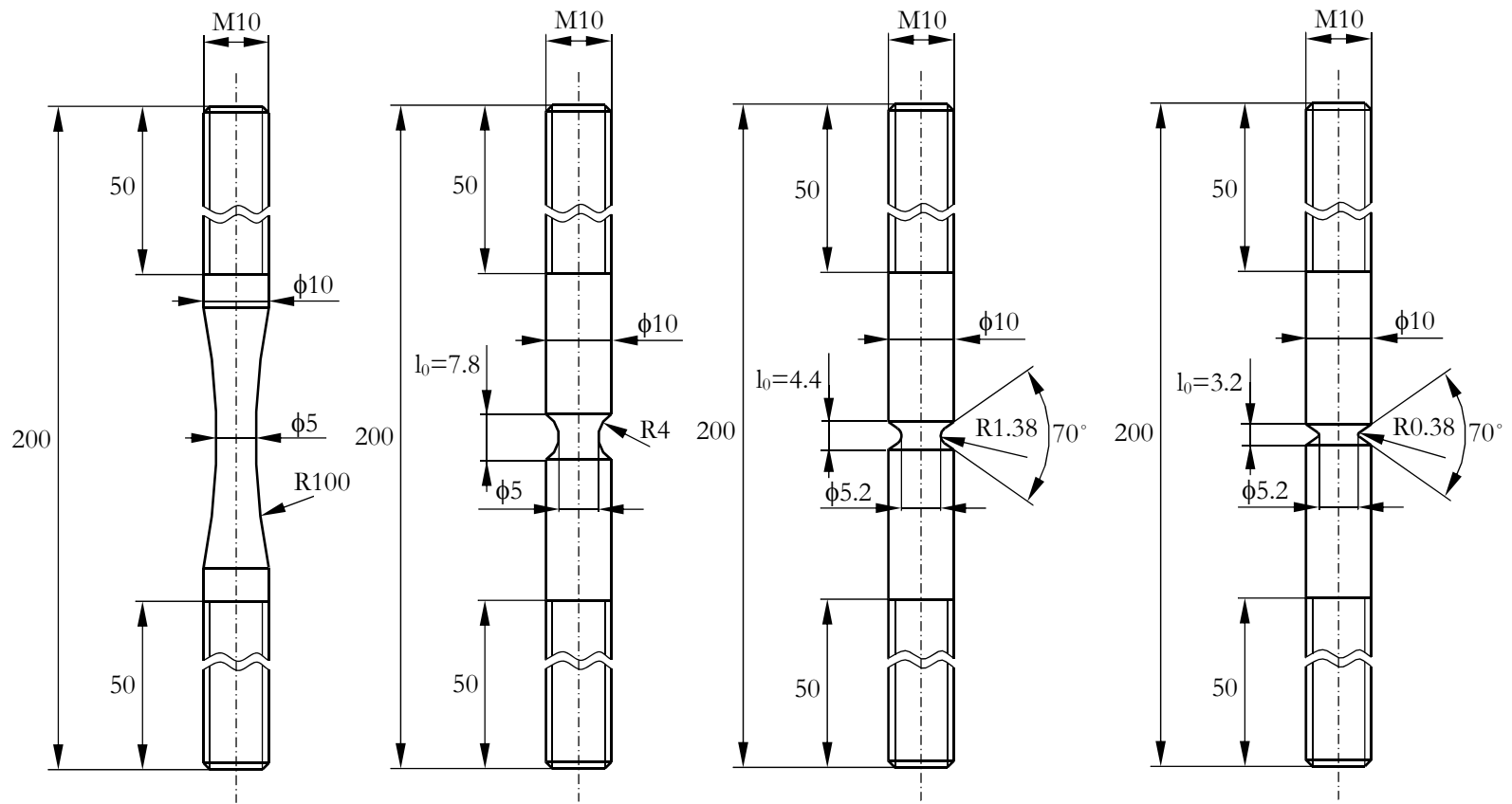
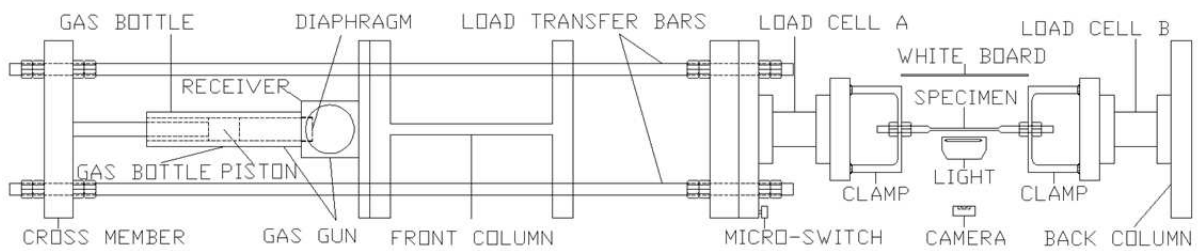
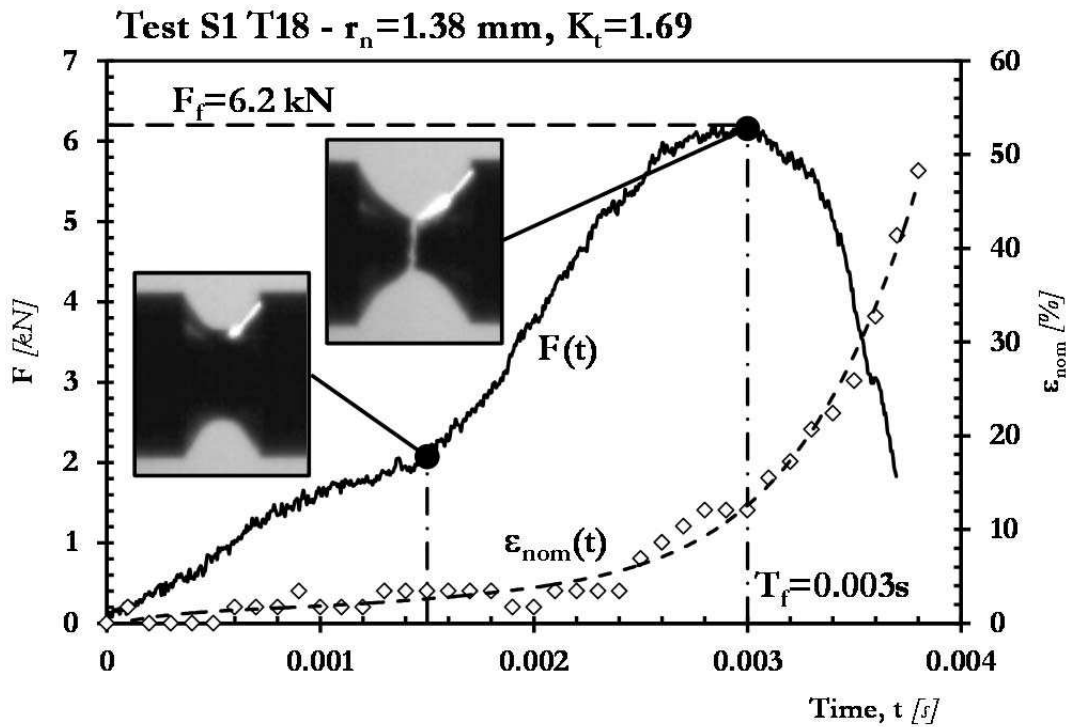


Figure 3. Geometries of the samples of Al6063-T5 tested at the University of Sheffield (dimensions in millimetres).



(a)



(b)

Figure 4. Experimental rig used to test the notched cylindrical samples of Al6063-T5 (a); force vs. time and nominal strain vs. time curve for test S1 T18 (b).

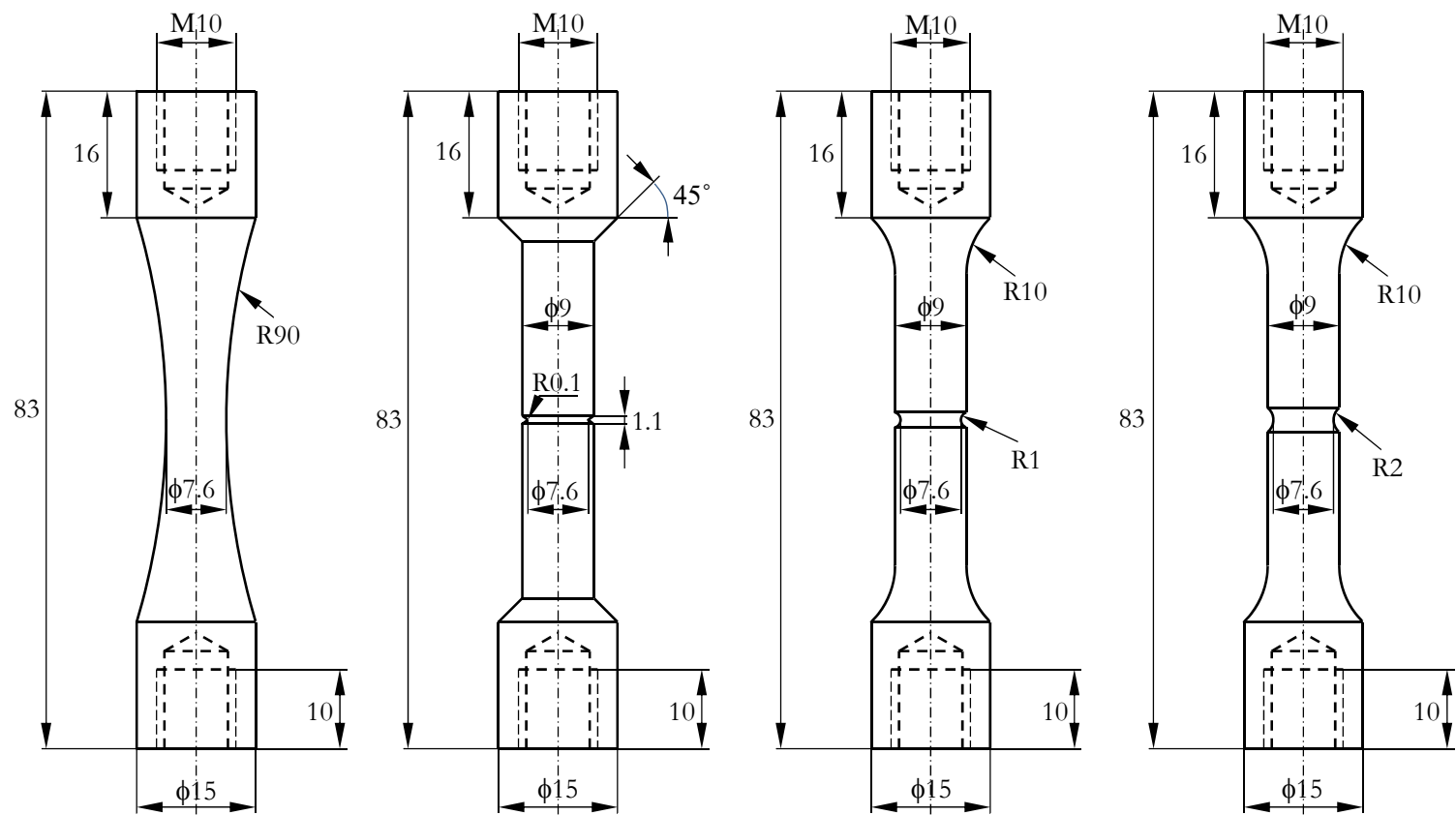


Figure 5. Geometries of the samples tested in the laboratory of the Institute of Continuous Media Mechanics UB RAS, Perm, Russia (dimensions in millimetres).

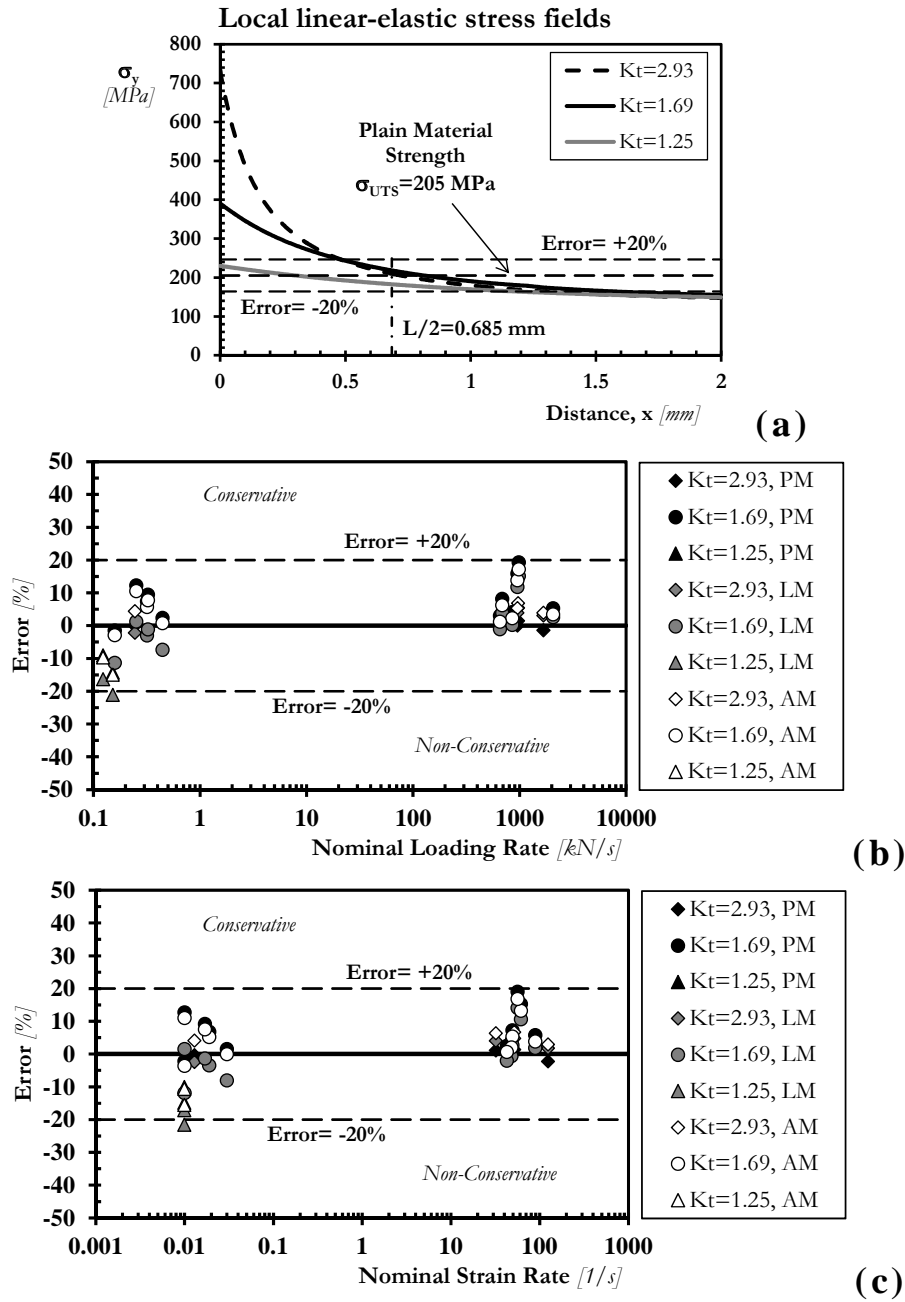


Figure 6. Local linear-elastic stress fields, in the incipient failure condition, under quasi-static loading ($\dot{F} \approx 0.15$ kN/s, $\dot{\epsilon}_{nom} \approx 0.01$ 1/s) for notched Al6063-T5 (a); accuracy of the TCD applied in terms of both loading rate (b) and nominal strain rate (c) in predicting the strength of notched Al6063-T5.

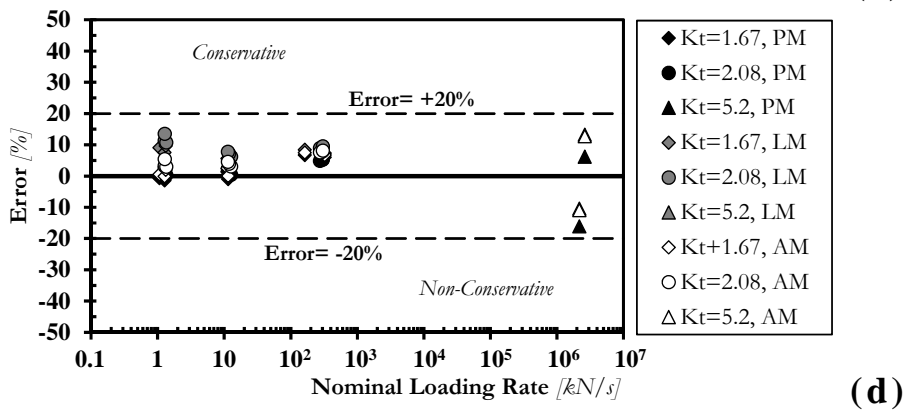
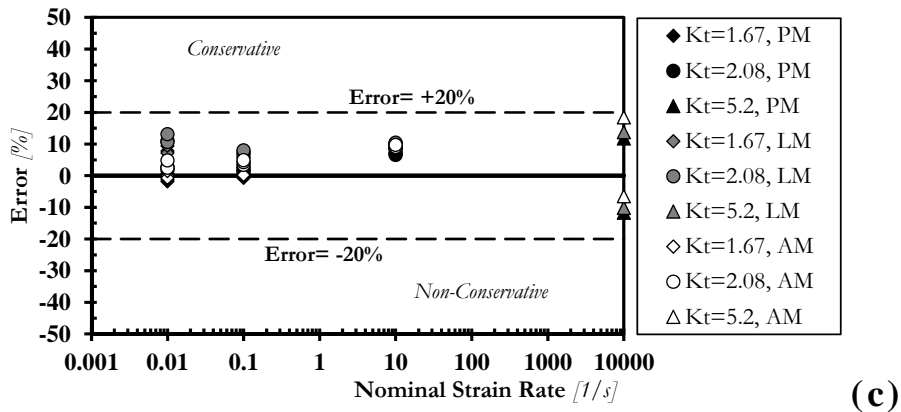
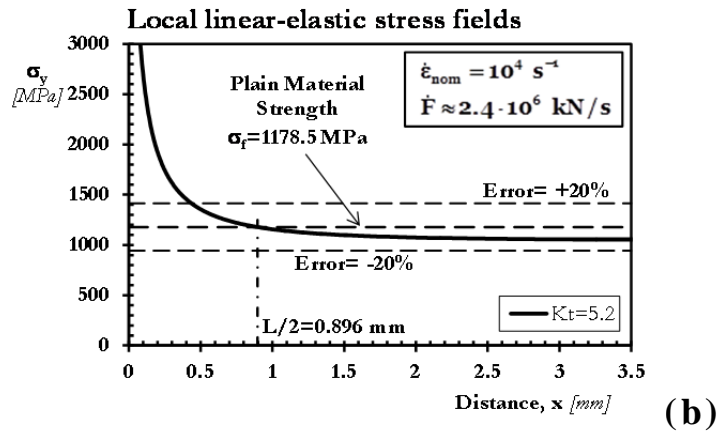
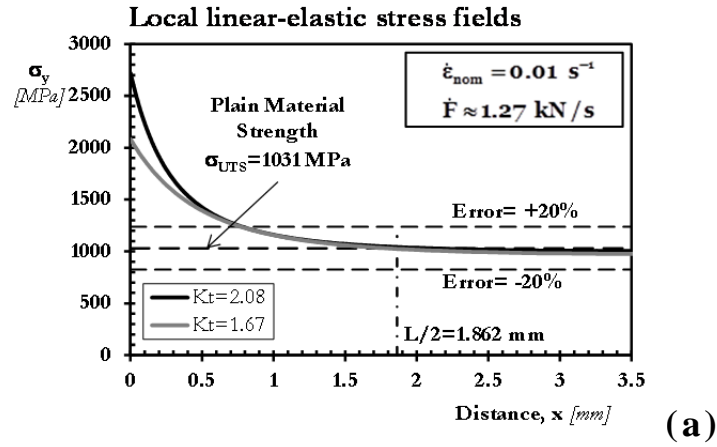


Figure 7. Local linear-elastic stress fields, in the incipient failure condition, under $\dot{\epsilon}_{nom} = 0.01$ 1/s (a) and $\dot{\epsilon}_{nom} = 10^4$ 1/s (b) for notched Ti-6Al-4V; accuracy of the TCD in predicting the strength of notched Ti-6Al-4V (c, d).

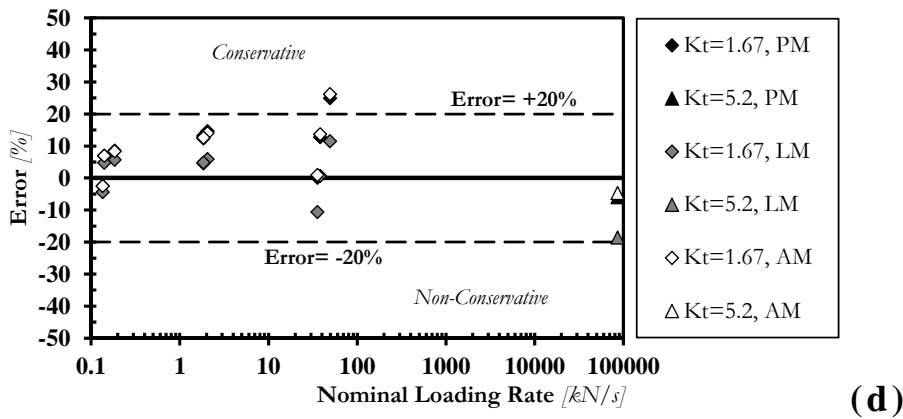
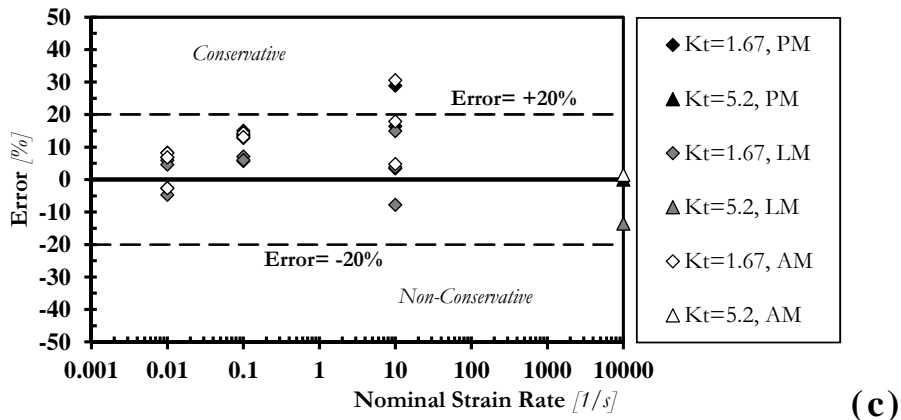
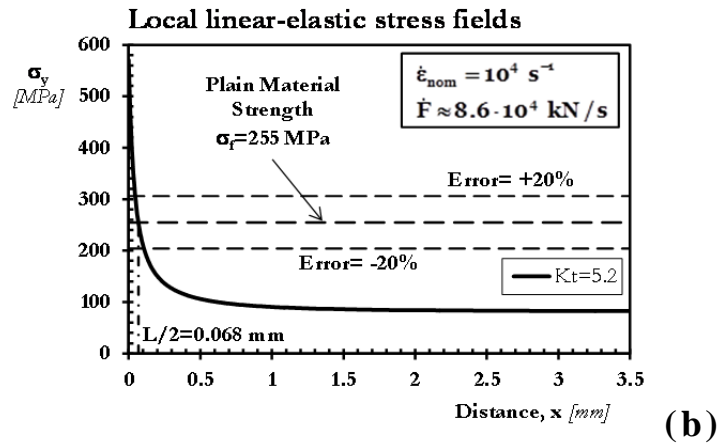
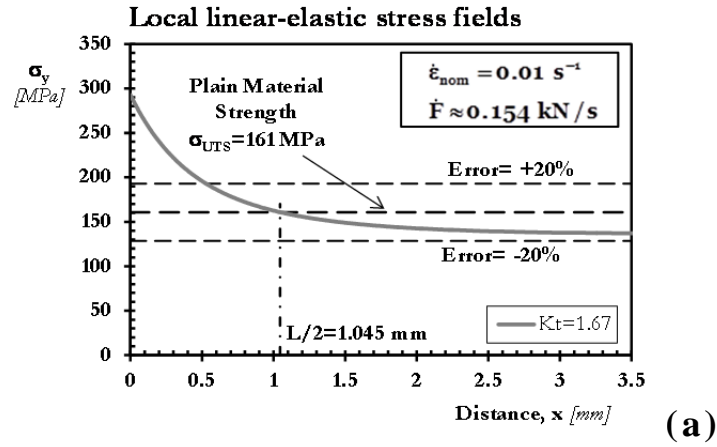


Figure 8. Local linear-elastic stress fields, in the incipient failure condition, under $\dot{\epsilon}_{nom} = 0.01 \text{ 1/s}$ (a) and $\dot{\epsilon}_{nom} = 10^4 \text{ 1/s}$ (b) for notched AlMn alloy; accuracy of the TCD in predicting the strength of notched AlMn alloy (c, d).

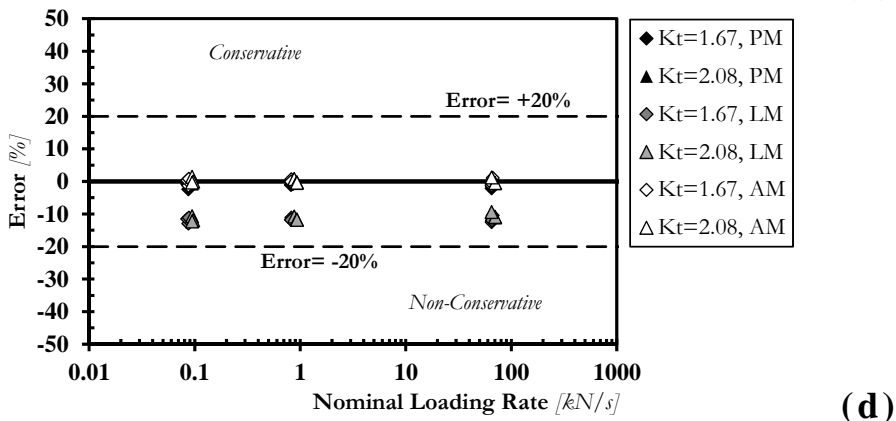
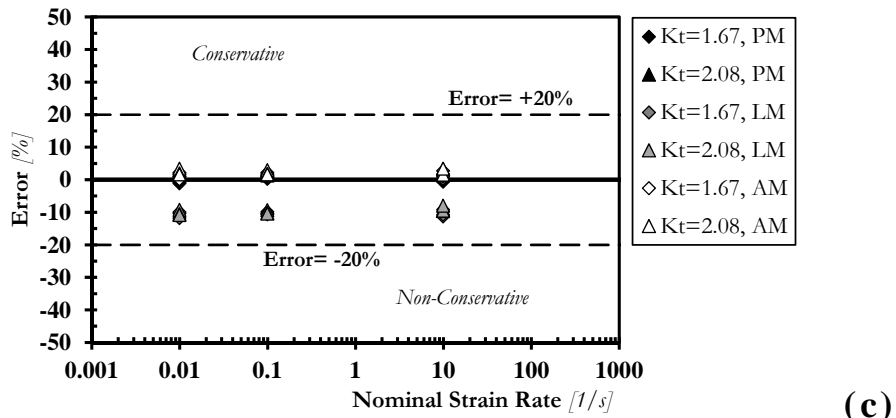
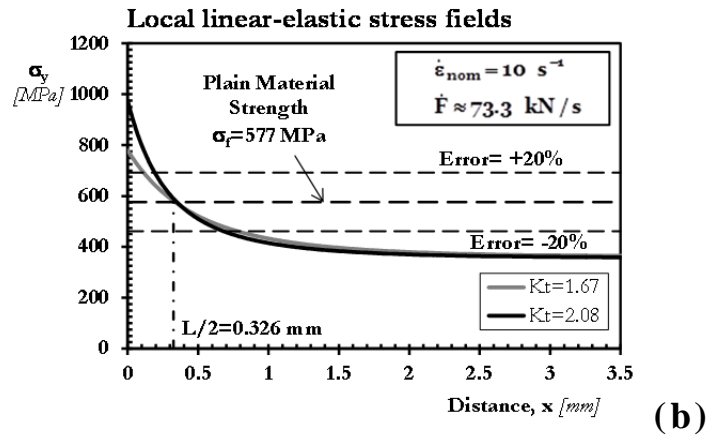
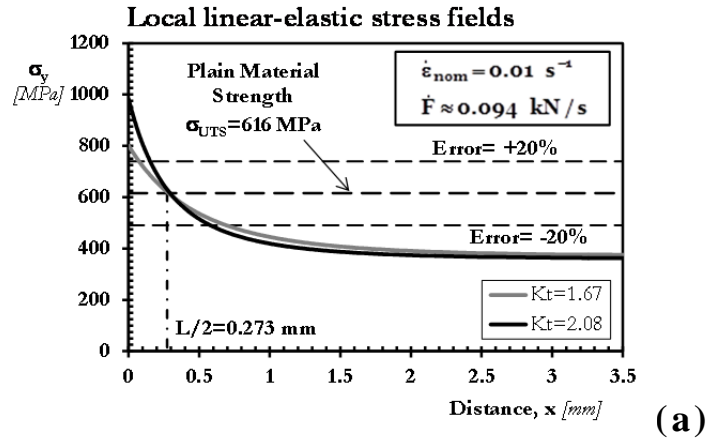
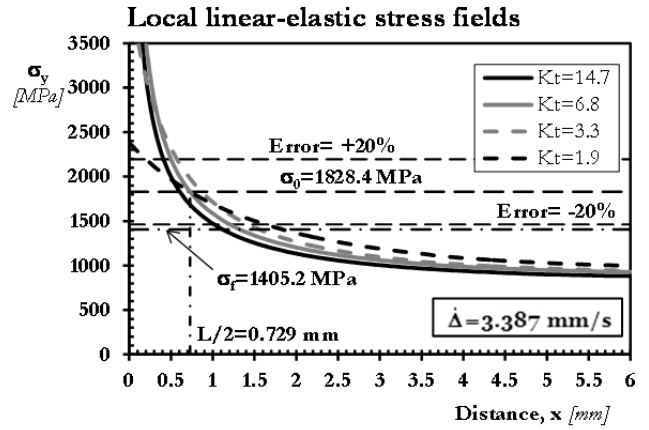
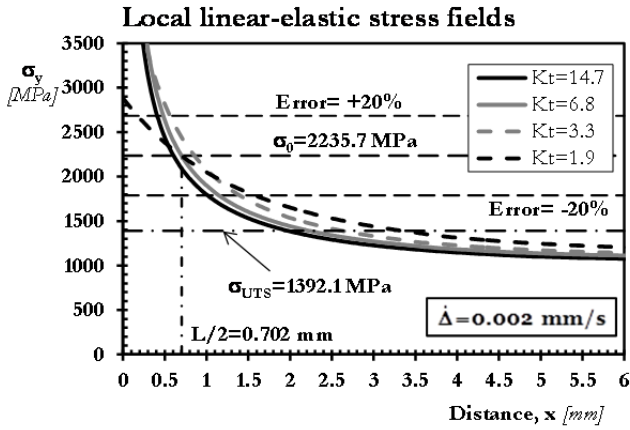
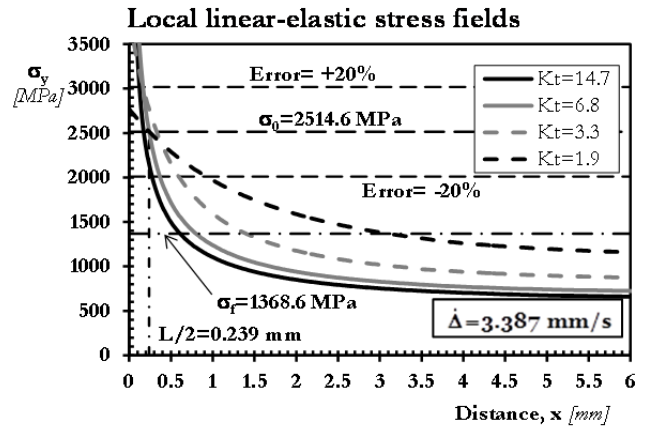
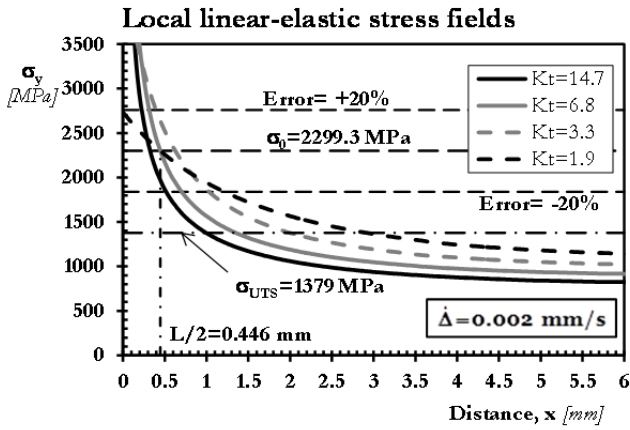


Figure 9. Local linear-elastic stress fields, in the incipient failure condition, under $\dot{\epsilon}_{nom} = 0.01$ 1/s (a) and $\dot{\epsilon}_{nom} = 10^4$ 1/s (b) for notched AlMg6; accuracy of the TCD in predicting the strength of notched AlMg6 alloy (c, d).

30 1XH Stainless steel



René-41 Alloy



Jet-1000 Steel

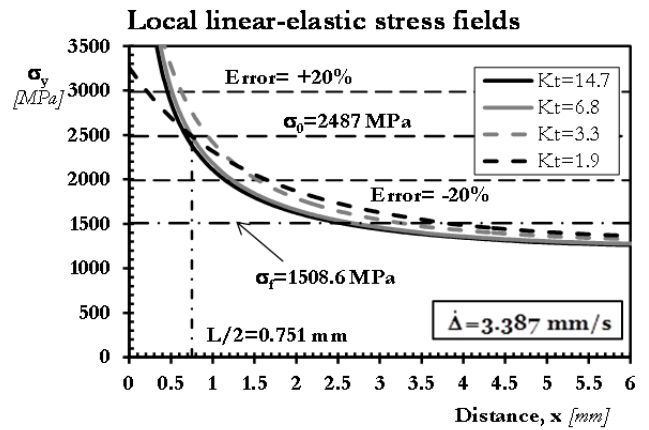
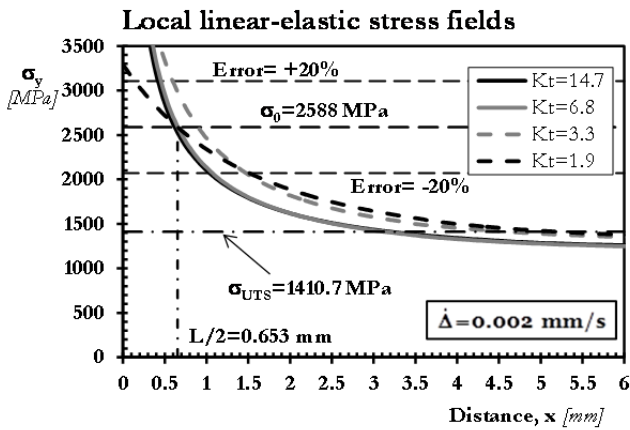


Figure 10. Local linear-elastic stress fields, in the incipient failure condition, under $\dot{\Delta} = 0.002$ mm/s and $\dot{\Delta} = 3.387$ mm/s for notched metallic materials 301XH, René-41, and Jet-1000 (data taken from Ref. [51]).

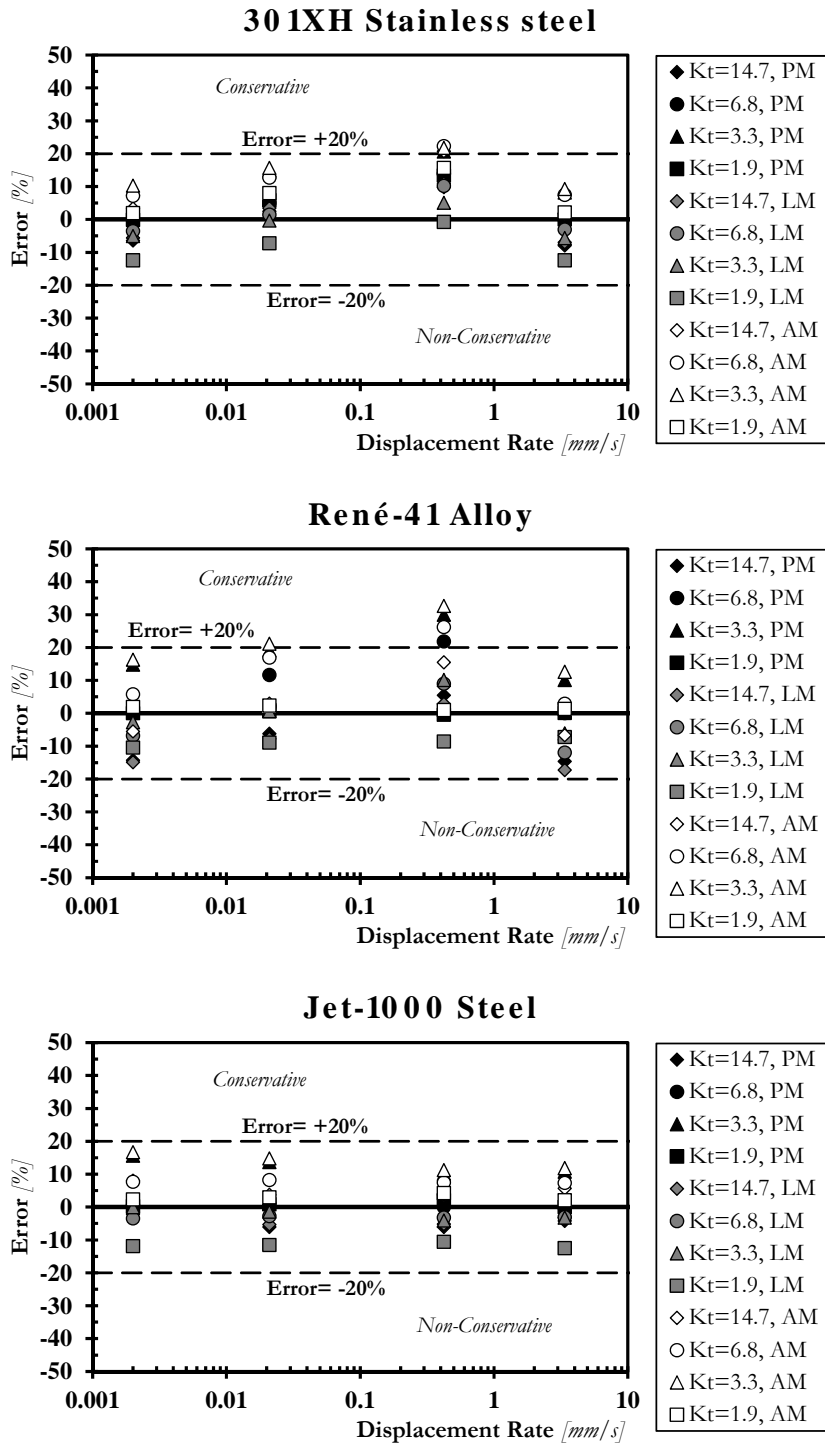


Figure 11. Accuracy of the TCD in predicting the strength of notched metallic materials 301XH, René-41, and Jet-1000 (data taken from Ref. [51]).